Utility of Satellite-Derived Burn Severity to Study Short- and Long-Term Effects of Wildfire on Streamflow at the Basin Scale

Hernan A. Moreno[1*], Jonathan J. Gourley[2], Tri G. Pham[3], Daniela M. Spade[1],

1. Department of Geography and Environmental Sustainability
University of Oklahoma
Sarkeys Energy Center
Norman, OK 73072
USA

2. NOAA/National Severe Storms Laboratory
120 David L. Boren Blvd.
Norman, OK 73072
USA

3. School of Civil Engineering and Environmental Science
University of Oklahoma
Sarkeys Energy Center
Norman, OK 73072
USA

Submitted to *Journal of Hydrology*
July 2019

---

* *Corresponding author address*: Hernan A. Moreno, Department of Geography and Environmental Sustainability, University of Oklahoma. 100 East Boyd St, SEC Suite 662, Norman OK 73019, Tel +1 480 399-0571, email moreno@ou.edu

Abstract

We investigated the changes in hydrologic response in a forested catchment impacted by wildfire in Colorado U.S.A. from the storm event to the inter-annual scales. We also evaluated the utility of a remotely-sensed burn severity index to study post-fire shifts in streamflow. At the storm-scale, we evaluated hydrologic shifts through changes in the effective runoff (Q^*/P_{Tot}), peak streamflow (Q_{pk}) and response time (T_R/T_B) from multiple hydrographs, while at seasonal and inter-annual-scales we quantified hydrologic shifts through the runoff fraction (Q/P_{Tot}) and flow duration curves. Vegetation anomalies were monitored through comparisons of the Normalized Burn Ratio (NBR) between the burned and a hydrologically-similar, forested, neighboring, unburned catchment. We found short-term acute and long-term chronic transient streamflow shifts from the minute to the inter-annual scales. Flow duration curves indicate an order of magnitude increase in maximum flows. Event-average Q^*/P_{Tot} increased by two orders of magnitude and Q_{pk} increased by one order of magnitude relative to multiple representative pre-fire events of similar precipitation intensities. Decreases in T_R/T_B appear to be minimal. At the inter-annual scale, increases in the difference between simultaneous unburned and burned NBR are associated with increases in Q/P_{Tot}. A hydrologic recovery pathway is evident resembling a hysteresis effect driven by vegetation re-growth. Results illustrate the non-steady physical processes that increase flash-flooding risks post-fire in mountainous catchments and the utility of ΔNBR as a hydrologic predictor in ungauged watersheds.

Keywords: Wildfire hydrology, remote sensing hydrology, Normalized Burn Ratio, Post-fire streamflow shifts, forest hydrology, land cover change.

1. Introduction

Quantifying the magnitude and temporal extent of streamflow shifts in recently burned mountain catchments is of primary interest due to the substantial increase in flash flooding and debris flow risks downstream of the burned areas. This task is particularly challenging in ungauged, topographically-complex catchments prone to intense, convective precipitation. A significant amount of research has been devoted to this topic, and several site-specific factors such as regional climate (Zhou et al., 2015), watershed terrain characteristics (Wine and Cadol, 2016), burn area and severity (Moody et al. 2007; Benyon and Lane, 2013), and vegetation species (Kuczera, 1987; Heath et al., 2014) have been found to result in varying degrees of streamflow shifts in magnitude and longevity (Kinoshita and Hogue, 2015). Despite previous work on using remote sensing indices to investigate changes in runoff production, the utility of NBR to infer both short- and long-term hydrologic changes has not been fully evaluated. Linking vegetation burn severity and hydrologic anomalies becomes a relevant topic for water and land managers that often require site-specific information on the expected duration and magnitude of fire-induced streamflow shifts.

Post-fire streamflow shifts have occurred globally across various climatic conditions and spatiotemporal scales but mostly in the U.S western states of California (Bart and Hope, 2010; Kinoshita and Hogue, 2015; Bart, 2016), New Mexico (Wine and Cadol, 2016), and Colorado (Larsen et al., 2009), and also in Portugal (Walsh et al., 1994), Spain (Cerdà and Lasanta, 2005), Israel (Inbar et al., 1998), and Australia (Zhou et al., 2015). Three streamflow metrics are usually investigated as indicators of hydrologic anomalies: (1) runoff volume (Helvey, 1980; Moody et al., 2008; Moody and Ebel, 2014; Ebel et al., 2012); (2) peak streamflow (Moody and Martin, 2001b; Shakesby and Doerr, 2006); and (3) time to peak streamflow (Neary et al., 2005). Post-fire runoff shifts have been evaluated from the plot (Benavides-Solorio and MacDonald, 2001) to the catchment scale (Moody et al., 2008). Such changes in runoff production generally occur because of the formation or enhancement of water-repellant soils (DeBano, 2000) as well as significant decreases in vegetation density and litter cover (Cerdà and Doerr, 2005). The post-fire conditions enhance infiltration-excess runoff mechanisms (Shakesby and Doerr, 2006) that result in positive peak streamflow shifts (Gottfried et al., 2003; MacDonald and Huffman, 2004; Stoof et al., 2012; Mahat et al., 2016; Moreno et al., 2016) and shorter response times (Baker et al., 2004; Neary et al., 2005; Cydzik and Hogue, 2009).

Fire severity effects on vegetation and soil properties and their subsequent recovery play a significant role in the short- (acute) and long-term (chronic) hydrologic responses of a burned region (Cerdà, 1998). In the case of long-term behavior, the post-fire hydrologic restoration rates can vary from year-to-year depending on regional climatic and vegetation conditions (Shin et al., 2013). Previous studies have noted the strong coupling between soil, vegetation and hydrologic recovery pathways, usually finding this process to occur within 2 to 7 years post-fire, in tandem with the re-establishment of vegetation, stream-network connectivity and soil hydraulic properties (Moody and Martin, 2001b; Cerdà and Doerr, 2005; Wittenberg et al., 2007; Mayor et al., 2007), although in certain cases it may take longer. For instance, Kinoshita and Hogue (2015) found elevated stream discharge during low flow seasons nearly ten years following a Californian wildfire, and attributed the elevated runoff to reduced transpiration.

Remote sensing indices are used to investigate the severity and track recovery pathways after wildfires. Among commonly used indices to study ecosystem damage after fire are the Enhanced Vegetation Index (EVI), the Normalized Difference Vegetation Index (NDVI) and, the more recently developed, Normalized Burn Ratio (NBR). All are usually computed from Landsat or MODIS imagery. Both EVI and NDVI were essentially developed to track canopy structural variations and health. Thereby, they can also be used to infer vegetation damage after fires (Wittenberg et al., 2007; Casady et al., 2010; Kinoshita and Hogue, 2011; Wine and Cadol, 2016; Uyeda et al., 2017). However, the application of EVI and NDVI to study post-fire vegetation alterations involves conceptual limitations related to the spectral bands that do not necessarily capture burn severity (Epting et al. 2005). Subsequently, the NBR was defined to identify and quantify the effects of fire on vegetation by including the mid-infrared band (Cocke et al. 2005, Epting et al. 2005, Roy et al. 2006, Walz et al. 2007, Loboda et al. 2007, Escuin et al., 2008, Weber et al. 2008). The difference between consecutive pre- and post-fire scenes (i.e ΔNBR) is usually taken to represent burn extent and severity (Miller et al. 2007, Moody et al, 2015). Despite recent advances in the understanding of the relationship between post-fire soil and vegetation recovery and the evolution of hydrologic shifts (Onda et al. 2008; Kinoshita and Hogue 2011), further research remains necessary at the catchment scale (Woodsmith et al., 2004) to relate the hydrologic anomalies to remotely-sensed imagery using paired-basin approaches. Innovations are particularly germane for application to ungauged basins.

Post-fire hydrologic shifts beyond the plot and hillslope scale were studied by several authors (Lane et al., 2006; Mayor et al., 2007; Heath et al., 2014; Wine and Cadol, 2016;

Bart and Hope, 2010; Bart, 2016). However, catchment scale studies are less frequently found than plot or hillslope scale investigations, and consequently streamflow dynamics at the watershed scale are less clearly understood under post-fire conditions (Moody and Martin, 2001a; Mayor et al., 2007). Furthermore, there is a paucity of post-fire studies with hydrological records available both pre- and post-fire (Woodsmith et al., 2004; Kinoshita and Hogue, 2015), making it difficult to quantify streamflow shifts relative to unburned conditions.

This study investigates catchment-scale hydrological shifts relative to unburned conditions at a predominantly forested catchment in Colorado, USA. The broader research questions are: (1) what are the potential links between basin-average NBR and the observed post-fire streamflow anomalies? And (2) how could paired-basin ΔNBR be used to quantify inter-annual runoff alterations and hydrologic recovery post-fire? The focus of the study is on the use of remote-sensing data to detect and track a basin's hydrologic response to wildfire impacts and to investigate the links with streamflow shifts through process-based analyses. Pre- and post-fire catchment observations of precipitation, streamflow and satellite-derived NBR are used. ΔNBR is computed from simultaneous burned and unburned paired catchments, with the purpose of excluding the effects of vegetation phenology, to infer changes due to the fire impacts that result in runoff generation shifts.

To account for the effects of severe weather within this mountain watershed, analyses are conducted under warm-season precipitation as measured by rain gauges situated within and nearby the catchment. Six years pre- and post-fire are analyzed as a representative period for precipitation and streamflow in regards to vegetation recovery, while also ensuring a representative number of storm events to synthesize hydrologic patterns.

The objectives of this study are to: (1) evaluate the utility of NBR in estimating transient shifts in runoff fraction, peak streamflow and time to peak streamflow, and (2) examine the coupled ecosystem-hydrologic response post-fire from the event to the inter-annual scale by combining ground stations and remote-sensing image analysis. The focus will be on the Camp Creek catchment located within Waldo Canyon in Colorado. Table 1 summarizes previous research and reports that have investigated the hydrological and societal impacts of the 2012 Waldo Canyon fire in Colorado, a unique and widely studied fire which also serves as a case study in the current paper.

Table 1: Summary of previous research concerning the 2012 Waldo Canyon fire.

Study/Report	Study area	Summary of findings
Verdin et al., 2012	22 basins affected by the Waldo Canyon burn scar	Model projected debris flow probabilities for Camp Creek were 24%, 45% and 55% for 2-year, 10-year, and 25-year storms, respectively.
Young and Rust, 2012	5 watersheds and 26 pour points within Waldo Canyon burn scar	Moderate and high severity burns occur on steep slopes, producing projected erosion rates of up to 31 t/ha for a 2-year runoff event, 61 t/ha for a 5-year event and 90 t/ha for a 10-year event.
Rosgen et al., 2013	Four major watersheds affected by the Waldo Canyon fire (including Camp Creek)	Projected annual change in water yield of 66 mm in Camp Creek due to reduction in forest cover. Comparisons of pre- and projected post-fire water yield indicates an increase in water yield by $1.95*10^6$ m^3 in Camp Creek. Project slow vegetative recovery rate due to coarse textured soils and low precipitation magnitudes relative to potential evapotranspiration.
Staley et al., 2015	12 drainage basins within Waldo Canyon burn scar	Total rainfall for debris-flow producing flash floods ranged from 7.2-34.9 mm with storm durations spanning from 10-125 minutes. Flash floods occurred following short bursts of high intensity rainfall events.
Kinoshita et al., 2016	Colorado Springs, CO	Hazard mitigation techniques often confound interrelated post-fire processes, thereby hindering predictions of post-fire natural responses.
Chin et al., 2016	Waldo Canyon burn scar	Barriers installed to block post-fire debris flow facilitated downstream erosion and channel degradation thereby enhancing the hazard and requiring further alterations to the landscape.

2. Study area, hydrology and remote sensing data

2.1 Wildfire coverage and study area

Between June 23rd and July 10th of 2012, the Waldo Canyon fire burned over 74 km^2 of land near Colorado Springs, CO. The wildfire extent, general area topography and vegetation distribution are shown in Figure 1 and Appendix A.1. The proximity of the fire to a large city (Colorado Springs, Figure 1) enhanced the human impact of the Waldo Canyon fire, damaging 346 homes and killing two people (City of Colorado Springs, 2013). The U.S. Forest Service's Inter-Agency Burn Area Emergency Response (BAER) team classified 28% of the burn area as very low severity, 23% as low, 29% as moderate and 20% high severity (see Figure A.1). Camp Creek is a 24.4 km^2 catchment with 78% of its drainage area affected by this fire (see Figure 1). Table 2 summarizes wildfire spatiotemporal characteristics within Camp Creek, indicating burned area and wildfire period.

Table 2: Wildfire characteristics in Camp Creek and hydrologic evaluation periods.

Feature	**Value**
Burned area [km^2]	19
% Catchment area burned	78
Unburned area [km^2]	5.4
Wildfire period	Jun 23 – Jul 10, 2012
Hydrologic evaluation period	Apr 2006 – June 2018
Pre-fire evaluation period	Apr 2006 – June 2012
Post-fire evaluation period	July 2012 –June 2018

According to the BAER team, Camp Creek had 36% of the burn area as low severity, 37% moderate severity and 5% high severity (Young and Rust, 2012; Rosgen et al., 2013). A neighboring unburned control catchment with similar topographic, channel network and land cover characteristics is Stanley Creek. This is a 9 km^2 watershed located within 8.7 km distance from Camp Creek that was used as a control catchment for comparing unburned to burned (i.e. Camp Creek) NBR values (see Figure 1).

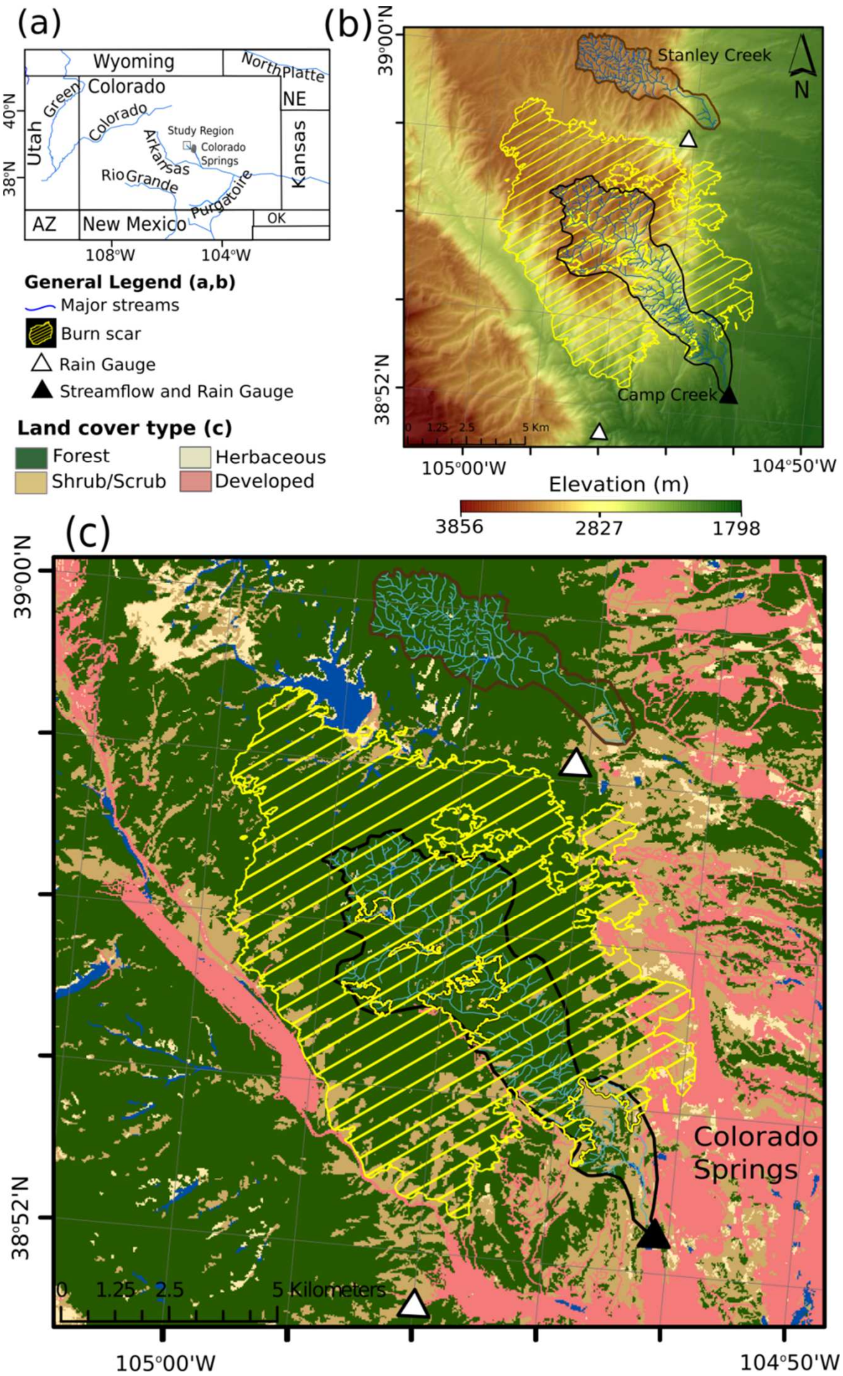

Figure 1: (a) Regional location of the study area including the Waldo Canyon fire near the Colorado Springs city limits. (b) General relief and channel network distribution at Camp Creek (burned) and Stanley Creek (unburned) catchments. (c) Land cover type at Camp Creek (burned) and Stanley Creek (unburned) catchments. On panels (b) and (c), burned areas are hatched in yellow. Also shown within the main legend are the used USGS and NOAA rain and streamflow gauge stations.

Table 3 documents geomorphic and land cover characteristics of the two (burned and unburned) catchments. Table 3 and Figure 1 indicate that both Camp and Stanley Creeks hold similar relief, channel network distribution, mean slope, general aspect and vegetation cover. Additionally, given the short distance that separates them, they share similar climates. Such similarities result in similar spectral signatures of the NBR (see section 4.1). The seasonality of precipitation in Colorado's central mountains is complex, with intense precipitation possible all year. However, during the warm season (April to October) the precipitation is likely to be convective and, even under unburned conditions, it can trigger instantaneous flood risk that is enhanced by the steep slopes of this region (Mahoney et al., 2015; Moreno et al. 2012, 2013).

Table 3: Topographic, land cover and hydrologic characteristics for Camp Creek (burned) and Stanley Creek (unburned) catchments. Seasonal and annual averages span from 2006 – 2018. Stanley Creek does not have a streamflow gauge or in-catchment rain gauge, and therefore only topographic and vegetation characteristics are reported.

Feature	Camp Creek (burned) catchment	Stanley Creek (unburned) catchment
Outlet coordinates	104.872° W, 38.875° N	104.890° W, 38.975° N
Total area [km^2]	24.4	9.0
Length of main channel [km]	13.8	8.3
Slope of main channel [mkm^{-1}]	127.4	95.1
Seasonal total precipitation [mm]	3960	-
Wettest season during study period	2015	-
Driest season during study period	2012	-
Annual average streamflow [m^3/s]	0.030	-
Seasonal average streamflow [m^3/s]	0.052	-
Mean elevation [m]	2539	2670
Minimum/maximum elevations [m]	1917/2936	2112/2857
Std. elevation [m]	287.0	206.4
Mean slope [%]	20.6	14.01
Std. slope [%]	10.5	8.8
Slope aspect (%)	SE 18.38 E 17.13 S 15.31 NE 13.16	E 22.91 SE 15.27 NE 14.92 S 12.43
Major vegetation class 1 (% area)	Evergreen Forest (77.5)	Evergreen Forest (84.5)
Major vegetation class 2	Shrub/Scrub (11.8)	Deciduous Forest (7.3)
Major vegetation class 3	Deciduous Forest (4.5)	Shrub/Scrub (6.2)
Kirpich (1985) Concentration time [min]	66.3	50.4

2.2 Observed precipitation and streamflow data

This study uses multi-year data from three precipitation gauges and one streamflow gauge spanning the warm season (April through October, without snow events) in the analysis of pre- and post-fire hydrologic patterns to emphasize rainfall-driven responses. Figure 1 shows the regional location of the study gauge stations while Table 4 illustrates station codes, type, measurement frequency and missing data, and Table 2 specifies the evaluation periods according to the data availability.

Table 4: Precipitation and streamflow gauges used in this study.

Code	Type	Time Step	% Missing data
USGS 07103703	Streamflow	15 min	0.52
USGS 07103703	Precipitation	5 min	2.6
USGS 07103800	Precipitation	5 min	5.7
NOAA COOP055352	Precipitation	1 hour	1.3

Camp Creek's main stream is ephemeral, with zero flow values outside of active precipitation events. It has 15-minute streamflow and 5-minute precipitation data available through the United States Geological Survey (USGS) National Water Information System and National Oceanic and Atmospheric Administration (NOAA) Cooperative Observer Program (COOP).

2.3 Remote sensing data

This study uses MOD13Q1 MODIS imagery to calculate the NBR and quantify fire-induced changes within the burned (Camp Creek) relative to the unburned (Stanley Creek) catchment. While EVI and NDVI are based on near infrared and visible light to quantify vegetation's density and health, NBR enhances the distinction between burned and unburned surfaces with the addition of the mid-infrared spectral band. The MOD13Q1 MODIS provides imagery for calculating 16-day composites of NBR data at

250-m resolution and is available from February 2000 – present (NASA LP DAAC, 2000).

3. Methods

3.1 Evolution of catchment burn severity and streamflow pre- and post-fire

NBR values were calculated from the near-infrared (NIR) and mid-infrared (MIR) MODIS bands (Roy et al., 2006) for both Camp and Stanley Creeks. The phenologic cycles in the spectral signal of vegetation prevent the use of a single- reference, pre-fire NBR image for Camp Creek to estimate NBR changes with respect to standard conditions. Instead, comparing simultaneous NBR composites at paired Camp Creek and Stanley Creek catchments helps in isolating the effects of fire on vegetation from natural variability. Therefore, a NBR time series analysis was conducted to determine if both (i.e. burned and unburned) catchment's spectral signal (mean and variability) preserved a high correlation coefficient during pre-fire conditions (Lhermitte et al., 2010; Veraverbeke et al., 2010; Diaz-Delgado and Pons, 2001; Veraverbeke et al., 2010). Further, regression analysis was applied (e.g. logarithmic, exponential, linear, power law, and polynomial) to best fit the first two distributional moments during the 2006 through 2012 period. The best predictor was used to adjust NBR values at Stanley to Camp Creek pre-fire and to forecast post-fire NBR at Camp Creek as if it was unburned. Catchment average and standard deviation NBR values associated with the burned and unburned conditions were computed throughout the April – October season over the evaluation period excluding any periods with observed snow on the ground. In a typical year, and for clear-sky conditions, a maximum of 14 average NBR composites (2 per month over the 7-month season) were available. ΔNBR was then computed as the difference between adjusted unburned and burned conditions at Camp Creek as illustrated by equation (1) (Diaz-Delgado and Pons, 2001):

$$\Delta NBR(t)=NBR_{unburned}(t)-NBR_{burned}(t) \tag{1}$$

Where t is the simultaneous period for which the difference is calculated. All terms represent catchment-average values. $NBR_{unburned}$ and NBR_{burned} correspond to the adjusted NBR from Stanley Creek and the simultaneous values at Camp Creek, respectively. Although this difference (i.e. ΔNBR) only makes sense post-fire, the calculation pre-fire should yield values close to zero, as a way to ensure that both adjusted and actual NBR values were very similar pre-fire. Theoretically, ΔNBR ranges from -2 (negative two) indicating healthier vegetation and 2 (positive two) for high severity burn with 0 (zero) meaning conditions similar to pre-fire. This methodology facilitated the tracking of post-fire vegetation recovery relative to the unburned conditions under similar climatic conditions.

Flow duration curves (FDCs) are widely used to study exceedance probabilities of mean and extreme hydrologic values. In some cases, they have also been used to evaluate the effects of catchment disturbances on flow distribution, providing statistical information on streamflow variability (Lane et al., 2005; Lane et al., 2006; Kinoshita and Hogue, 2015). FDCs were created for the pre- and post-fire study periods in Camp Creek using daily average streamflow data to identify fire-related shifts in streamflow frequency distribution.

3.2 Cross-scale temporal streamflow shifts

The subsequent event-scale analyses incorporated ΔNBR by using the average values associated with the closest-in-time 16-day composite of each month, depending on the date of the streamflow event. Similarly, the seasonal and inter-annual-scale analyses took the average of each year's 14 NBR composites to compute ΔNBR between the burned and unburned vegetation. Regarding the streamflow metrics, event, daily and seasonal scale values were computed to assess runoff changes post-fire relative to pre-fire conditions. Event-scale calculations were conducted for a total of 76 hydrologic events, 38 associated with pre-fire and another 38 with post-fire conditions. Table 2 summarizes the pre-fire and post-fire time spans. All periods with snowfall or presence of snow on the ground were removed from the analyses. To ensure that initial soil moisture conditions were low, events with minimal precipitation ($P \leq 3$ mm) five days prior were selected, so that the hydrologic effects due to land cover change, rather than high antecedent soil moisture, could be isolated. Figure 2 illustrates a typical response hydrograph where Q represents the total streamflow through the basin outlet as a result of both base flow, Q_B, and event flow, Q*. Q* represents the total water volume per unit catchment area as a result of the precipitation depth, P_{Tot}. A graphical base flow separation method was used to divide response hydrographs between Q_B and Q* (Figure 2; Dingman, 2015). At the monthly and seasonal scales, Q represents the total streamflow volume leaving the catchment through its outlet as a result of a monthly or seasonal precipitation input, P_{Tot}. Calculations for the monthly and seasonal Q and P_{Tot} are made for the months and seasons associated with each of the 78 maximum hydrologic events in Camp Creek.

Based on those streamflow metrics, four comparative streamflow response metrics were used: (a) event effective runoff per unit precipitation, Q^*/P_{Tot} (mm/mm), (b) event peak streamflow, Q_{pk} (m^3/s), (c) event time to peak fraction of hydrograph base time, T_R/T_B, (min/min) and (d) monthly and seasonal runoff coefficient, Q/P_{Tot} (mm/mm).

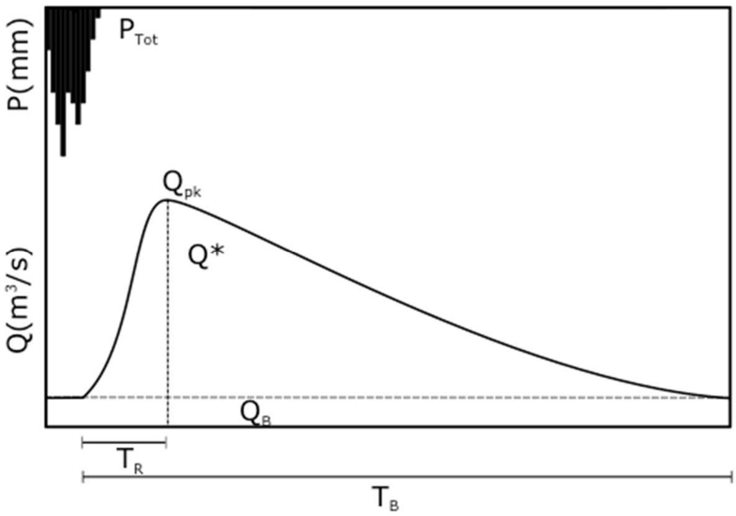

Figure 2: Typical watershed response hydrograph indicating how event flow (Q^*), total event precipitation (P_{Tot}), time to peak (T_R), time base (T_B) and maximum observed flow (Q_{pk}) are extracted. Q_B represents base flow.

High values of Q^*/P_{Tot} and Q_{pk} represent high runoff yields and maximum flows. Small values of T_R/T_B indicate a faster-paced hydrograph rise whereas larger values are associated with a slower rise. This cross-scale analysis facilitated the assessment of acute and chronic post-fire anomalies in runoff production per unit drainage area and precipitation depth so that runoff changes could be mostly attributed to vegetation alterations produced within the burn scars.

3.3 Streamflow shifts and burn severity links

In order to explore the co-dependence of $Q^*/P_{Tot,}$ Q_{pk} and T_R/T_B with event precipitation properties such as precipitation total (P_{Tot}), average and maximum intensity (I_{ave} and I_{max}) and land cover change due to burn severity (i.e. ΔNBR), a variance contribution approach was applied including the76 study events. First, scatterplots and correlation coefficients between pairs of I_{max}, P_{Tot} and I_{avg} were calculated to assess their level of independence prior to the application of the variance contribution analysis. Then $Q^*/P_{Tot,}$ Q_{pk} and T_R/T_B were plotted against ΔNBR with regards to their P_{Tot}, I_{max} and I_{avg} to investigate the potential links among groups of three variables (e.g. Q^*/P_{Tot}, ΔNBR and P_{Tot}). Empirical density distributions were plotted and Kolmogorov-Smirnov tests were conducted in regards to the pre- and post-fire distributions. Subsequently, a variance contribution analysis was conducted for variable arrays containing each of the event streamflow properties (Q^*/P_{Tot}, Q_{pk} and T_R/T_B) and all other independent variables including precipitation characteristics and ΔNBR (I_{max}, P_{Tot}, I_{avg} and ΔNBR). The method includes all measured predictors into multiple linear combinations to find a subset that explains the highest percent of the variance in the predictands. Best subsets (Heinze et al. 2018; Olejnik et al. 2010) is a technique that relies on exhaustive searches for the best groups of the variables using an efficient branch-and-bound algorithm. The procedure fits 2^P (i.e. 16) models, where P=4 is the number of predictors in the dataset. The Akaike information criterion (AIC; Akaike, 1973) and the coefficient of determination (R^2) facilitate model selection by providing an estimator of the relative quality of statistical models for a given set of data. Results are presented in pie charts, model regression plots and tables for pre- and post-fire events. Finally, inter-annual Q/P_{Tot} were analyzed relative to simultaneous ΔNBR values to identify recovery patterns of vegetation properties and their potential controls on runoff production at Camp Creek.

4. Results

4.1 Evolution of catchment burn severity and streamflow pre- and post-fire

A sequence of NBR field values from May 2012 (pre-fire month) and August 2012 (post-fire month) and their corresponding NBR_{May}-NBR_{Aug} difference illustrates the effects that fire had on vegetation in the Waldo Canyon region (See Figure 3). In Figures 3(a) and 3(b), NBR values range between -1 and 1 pre- and post-fire with an evident shift to negative values post-fire indicating removal of vegetation by fire. The NBR_{May}-NBR_{Aug} difference illustrates changes of up to 2 NBR units in the most severely burned areas of Camp Creek. The pre-fire average basin values of NBR (i.e. NBR_{May}) for Camp Creek and Stanley Creek are 0.24 and 0.29, respectively. For post-fire conditions, the average NBR_{Aug} for Camp Creek is -0.03 while the unburned value for Stanley is 0.36.

NBR regression analysis found that either linear, logarithmic or polynomial models provided the same coefficient of determination (R^2=0.80) between simultaneous catchment-average values at Camp and Stanley Creeks during the 2006 through 2012 (pre-fire) period (see Table B.1). A linear model was then selected to express NBR at Camp Creek as a function of the values at Stanley Creek as shown by Figures B.1 and B.2. This results in synthetic time series of NBR at Camp Creek as if it was unburned thereby facilitating the comparison of burned and unburned conditions for post-fire events within Camp creek.

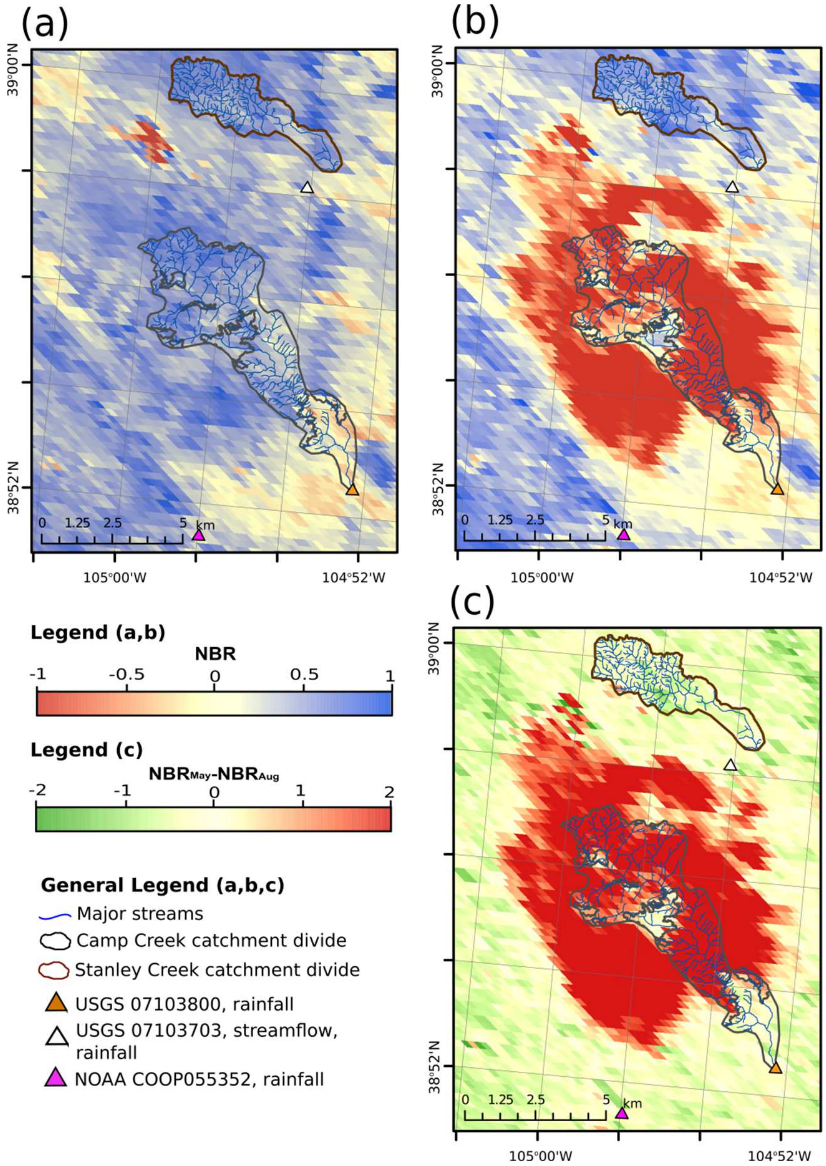

Figure 3: Spatial distribution of NBR during (a) pre-fire conditions in May 2012 and (b) post-fire conditions in August 2012. (c) Regional NBR_{May}-NBR_{Aug} difference for the Waldo Canyon including Camp and Stanley Creeks; negative values (green pixels) in the NBR_{May}-NBR_{Aug} difference map indicate healthier vegetation but positive (red pixels) indicate burn severity. Note that ΔNBR spans between -2 and 2 since NBR ranges from -1 to 1.

Time series of daily total precipitation P, bi-weekly mean and standard deviation NBR, and daily average streamflow Q, over Camp Creek catchment are shown in Figure 4 during the 12-year evaluation period. For reference, Stanley Creek's adjusted mean NBR time series have also been added to Figure 4. Seasonally, NBR peaks in late July and early August of each year. The Waldo Canyon wildfire abruptly decreases the post-fire Camp Creek's catchment-average NBR and increases its spatial variability as reflected by the larger standard deviation bars. However, after fire, NBR follows a recovery pathway gradually increasing each year. Further NBR's spatial variability appears to decrease faster returning to pre-fire values in about three years after the wildfire event.

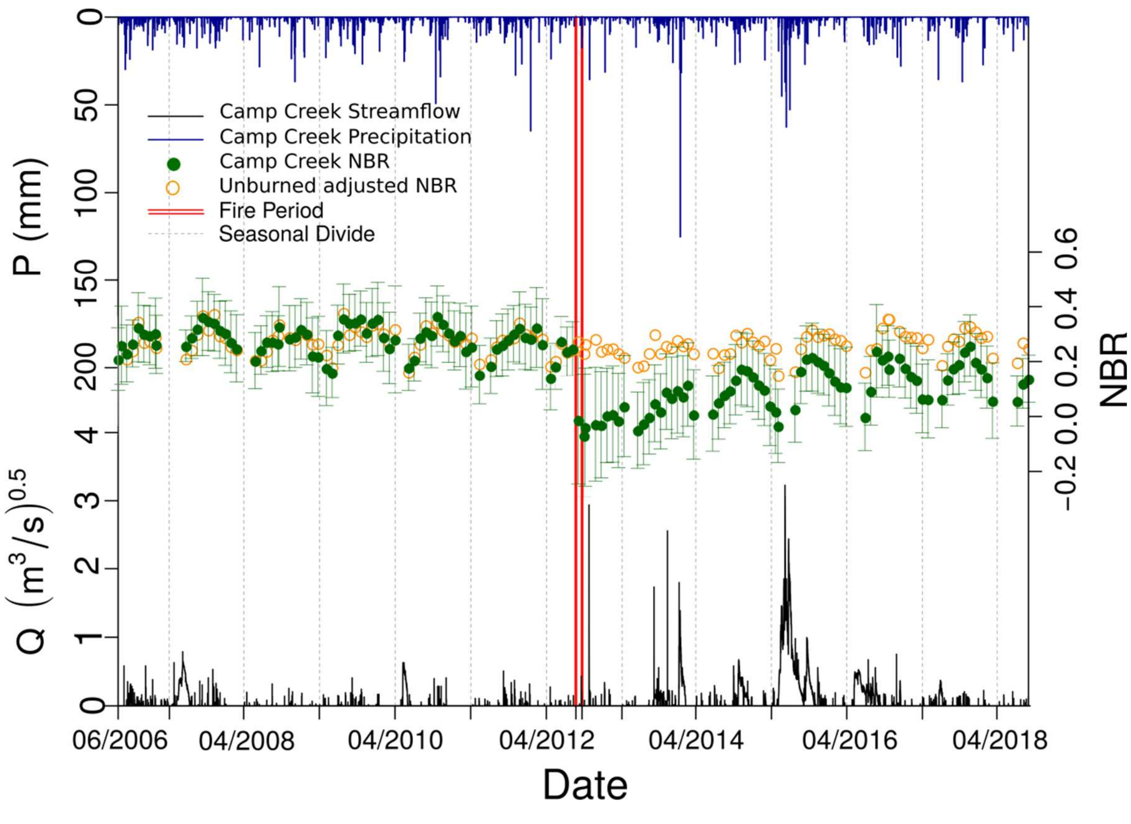

Figure 4: Time series of daily total precipitation (P, blue lines), daily average streamflow (Q, black lines) and monthly basin average and standard deviation of Normalized Burn Ratio (NBR, green dots and bars) for Camp Creek. Red lines represent the start and end of the Waldo Canyon wildfire. For reference, simultaneous catchment-average NBR values for Camp Creek predicted from the Stanley Creek time series have been added (hollow, orange circles). Q values are elevated to a 0.5 power with the purpose to better visualize the lowest flow rates.

In Camp Creek, the pre-fire (i.e. 2006-2012) and post-fire (i.e. 2012-2018) mean seasonal precipitation values were 357 and 416 mm, respectively. This difference can be explained by the exceptionally dry year of 2012 (year of the wildfire) with a precipitation total of 256 mm and the exceptionally wet year of 2015 with 663 mm of precipitation. In general, Camp Creek showed lower streamflow responses to precipitation events pre-fire (Figure 4). Changes in discharge are evident post-fire. The magnitude of streamflow events increased significantly post-fire, with the largest pre-fire Q_{pk} (over the 2006 – 2012 period) being 0.26 m^3/s while the largest post-fire Q_{pk} of 10.42 m^3/s occurred in May of 2015 (almost three years after the fire), equivalent to, at least, an order of magnitude increase with respect to the maximum Q_{pk} which occurred during the pre-fire period. Similar peak streamflow events occurred the same year and month after the wildfire in July of 2012 (8.64 m^3/s) and one year later in August of 2013 (6.54 m^3/s).

Warm-season flow duration curves (FDCs) are created from daily average streamflow data for the pre- and post-fire study periods and indicate changes in Camp Creek's flow regime post-fire (Figure 5). FDCs over a 20-year pre-fire time period (1992-2012) are used as the baseline to quantify fire impacts. Pre- and post-fire FDCs are not distributed over the entire range of exceedance probabilities because Camp Creek is an ephemeral stream. The rightward shift of the post-fire FDC indicates that all portions of the flow regime are affected by burn scars, and the streamflow at each probability value is, on average, an order of magnitude larger across the range of probabilities. High flows (flows at 1% exceedance probability; Smakhtin, 2001) increase from 0.74 m^3/s pre-fire to 2.5 m^3/s post-fire. Low flows (flows 99% exceedance probability; Brown et al., 2005) do not increase in magnitude, remaining at 0 m^3/s post-fire. However, the shift in streamflow distribution post-fire indicates that the number of zero flow days slightly decreased. Throughout the 20 years prior to the wildfire, zero flow days occurred 88.9% of the time and over the 6-year post-fire time span, this value decreased to 85.7% for a difference of 3.2% reduction in zero flow days.

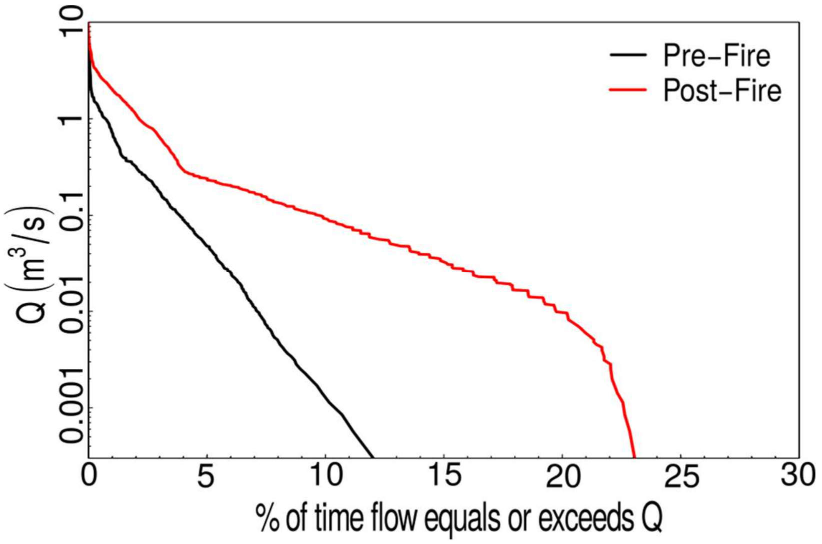

Figure 5: Pre- (black) and post- (red) fire flow duration curves for Camp Creek watershed computed from daily average streamflow data. Pre-fire flow duration curves were created using data from April 1992 – June 2012 and post-fire from July 2012 –July 2018.

4.2 Cross-scale temporal streamflow shifts

This section synthetizes the observed wildfire-induced streamflow shifts from the event to seasonal time scales. Figure 6 illustrates the pre- and post-fire Q^*/P_{Tot} for 76 hydrologic events (38 pre- and 38 post-fire) and their associated daily and monthly average Q/P_{Tot}. Symbols are colored by their corresponding total precipitation P_{Tot} (mm). A summary of the mean absolute and relative changes between pre- and post-fire values, at each temporal scale, is shown in Table 5.

Figure 6 and Table 5 indicate increases in effective runoff per unit precipitation from the event to the monthly time scales. Nonetheless, the largest difference in runoff between pre- and post-fire is observed at the event scale, with two orders of magnitude (i.e 10^2) higher values than pre-fire (see Table 5). Increases in streamflow magnitudes occur across a wide range of precipitation totals.

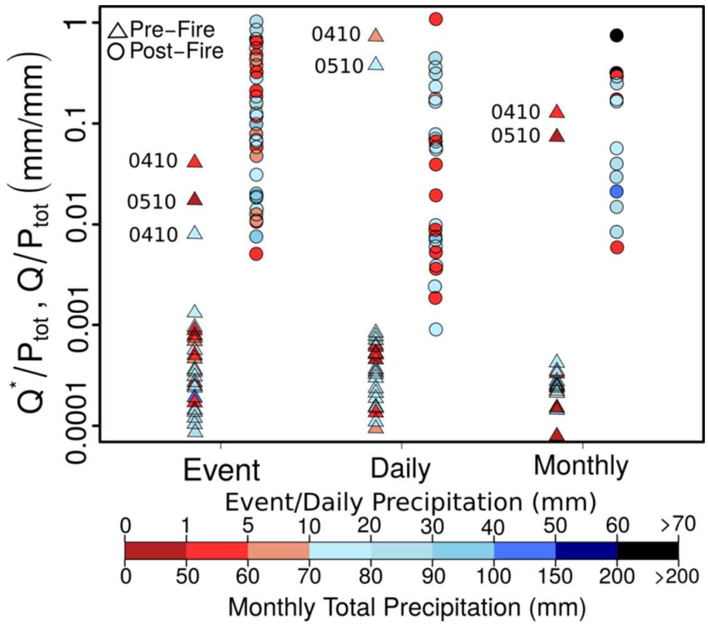

Figure 6: Q^*/P_{Tot} calculated at the storm and Q/P_{Tot} at the daily and monthly time scales for Camp Creek watershed. Triangles represent pre-fire and circles, post-fire hydrologic conditions. Labeling indicates the month (two-digit) and year (two-digit) when some large runoff pre-fire values occurred.

Table 5: Cross-scale average, absolute and relative mean differences of event Q^*/P_{Tot} and daily and monthly Q/P_{Tot} values for pre- and post-fire conditions.

Catchment	Temporal Scale	Pre-fire Average (mm/mm)	Post-fire Average (mm/mm)	Mean Absolute Change (mm/mm)	Relative increase (Post-fire/ Pre-fire)
	Event	0.0025	0.2131	+0.2168	1.1×10^2
Camp Creek	Daily	0.0349	0.1175	+0.0826	3.4×10^0
	Monthly	0.0135	0.1413	+0.1278	1.1×10^1

4.3 Streamflow shift links with burn severity

This section illustrates the differing hydrologic response patterns between pre- and post-fire conditions for individual precipitation events at Camp Creek and the role of burn severity on the observed acute (event) and chronic (inter-annual) streamflow shifts.

Figure 7 provides an example case of the corresponding response hydrographs for two such events that are similar in P_{Tot} and I_{avg}. Figure 7(b) illustrates a post-fire storm event with a P_{Tot} of 27.6 mm and I_{avg} of 6.12 mm/hr that produced a Q_{pk} of 8.64 m^3/s and a Q^*/P_{Tot} of 0.85. These values (i.e. Q_{pk} and Q^*/P_{Tot}) are, at least, one and two orders of magnitude, respectively, larger than the pre-fire values shown in Figure 7(a).

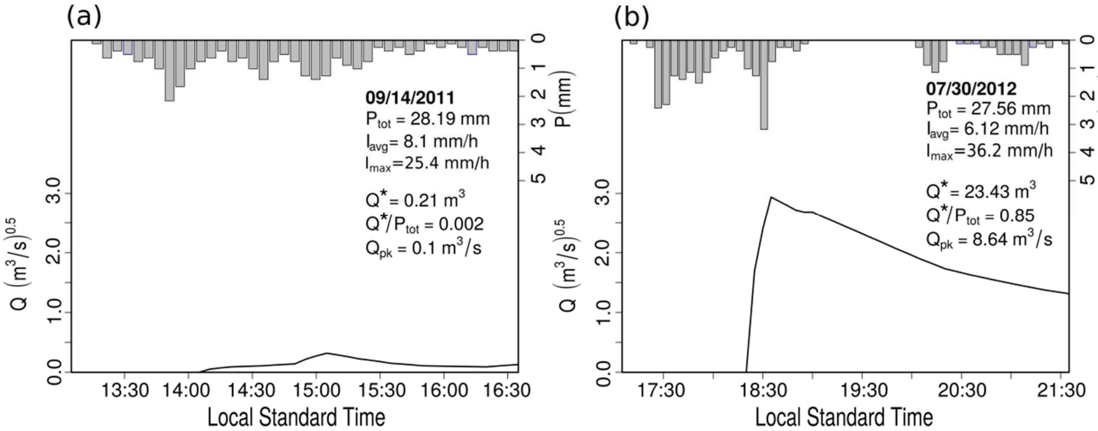

Figure 7: Example case hyetographs (5-min) and corresponding response hydrographs (15-min) for similar (i.e. I_{avg} and P_{Tot}) precipitation events before (a) and after (b) the Waldo Canyon fire at Camp Creek. Occurrence dates, total event precipitation (P_{Total}), mean precipitation intensity (I_{avg}), maximum 5-min precipitation intensity (I_{max}), event flow volume (Q^*), effective runoff fraction (Q^*/P_{Total}) and peak flow (Q_{pk}) values are indicated within each panel.

The total precipitation five days prior to each event is 1.2 mm pre-fire, and 3.1 mm post-fire, indicating that the antecedent soil moisture between the two events is similar. The nature and properties of precipitation play a definitive role on the magnitude and pace of the response hydrograph and this is the reason why the following results are illustrated in terms of I_{max}, I_{avg} and P_{Tot}.

To expand on the analysis of Q^*/P_{Tot}, Q_{pk} and T_R/T_B for the pre- and post-fire study events, Figure 8 illustrates their relationships with ΔNBR and classifies according to precipitation properties (i.e. P_{Tot}, I_{max}, I_{avg}) for the 76 pre- and post-fire storm events. To help understand average pre- and post-fire behaviors, Table 6 further synthetizes event-based mean, absolute and relative hydrograph shifts. From Figure 8 and Table 6, it can be inferred that, at the event scale, and for a wide range of P_{Tot}, I_{max} and I_{avg} values, increases in two orders of magnitude (i.e. 10^2) on Q^*/P_{Tot} are observed post-fire relative to pre-fire conditions. Similarly, increases of one order of magnitude (i.e. 10^1) on Q_{pk} occur, on average, across a large spectrum of P_{Tot}, I_{max} and I_{avg}. Additionally, T_R/T_B only shows a reduction of 10% relative to pre-fire conditions, illustrating a slight decrease on the average time to peak relative to pre-fire conditions.

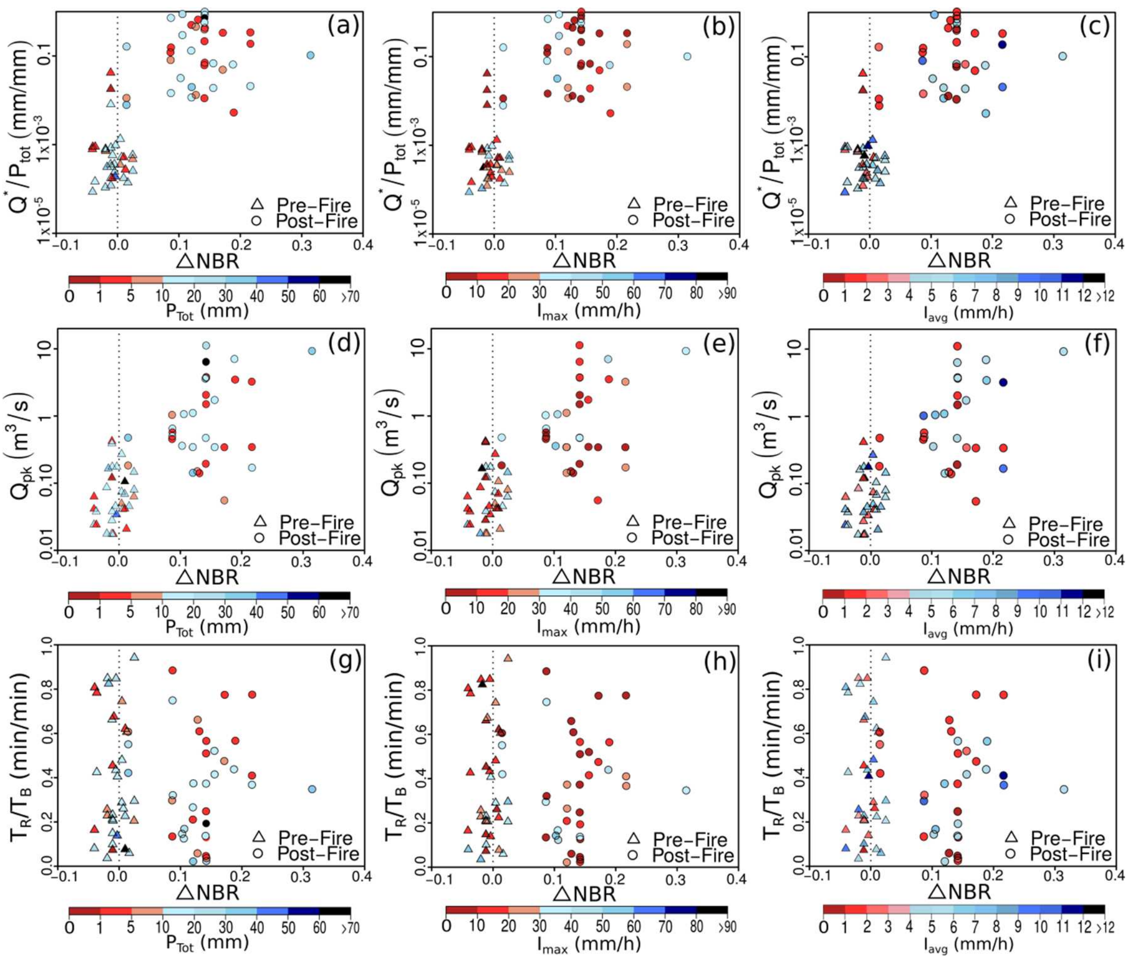

Figure 8: Event scale scatterplots of Q^*/P_{Tot}, Q_{pk} and T_R/T_B vs. closest-in-time ΔNBR values for Camp Creek during multiple isolated warm-season storm events. Hydrologic events are classified by P_{Tot} (mm; left-hand side column), I_{max} (mm/h; center column) and I_{avg} (mm/h; right-hand side column).

Besides ΔNBR, P_{Tot} and I_{avg} appear to contribute to the variability of all three streamflow metrics (i.e. Q^*/P_{Tot}, Q_{pk} and T_R/T_B) often regulating (i.e. enhancing or reducing) the effect of ΔNBR. For instance, for a moderate precipitation event (e.g. moderate P_{Tot} or I_{avg}) under a high ΔNBR, high Q^*/P_{Tot}, Q_{pk} and low T_R/T_B tend to occur. However, a similar situation will occur under moderate ΔNBR in the presence of high P_{Tot} and I_{avg}. Both scenarios result in an increase of streamflow values.

Table 6: Average Q^*/P_{Tot}, Q_{pk} and T_R/T_B at Camp Creek along with mean absolute and relative changes for all events shown in Figure 8 for pre- and post-fire conditions.

Metric	Pre-fire Event Average	Post-fire Event Average	Mean Absolute Change	Relative Change (Post-fire/ Pre-fire)
Q^*/P_{Tot} (mm/mm)	0.002	0.231	0.229	1.1×10^2
Q_{pk} (m^3/s)	0.090	1.678	1.588	1.9×10^1
T_R/T_B (min/min)	0.387	0.357	-0.03	0.9

A further look to the probability density functions (Figure 9) and Kolmogorov-Smirnov (K-S) tests (Table 7) illustrate that precipitation properties (e.g. P_{Tot}, I_{max}, I_{avg}) do not appear to change significantly from pre- to post-fire, except for a possible reduction in average intensity (I_{avg}; Fig 9 and Table 7) post-fire. Contrastingly, ΔNBR distributions and K-S test illustrate an evident right-ward (increasing) shift post-fire (Fig. 9(d) and Table 7). The density functions of post-fire Q^*/P_{Tot} and Q_{pk} are also right-shifted relative to pre-fire (Fig.9 (e), (f) and Table 7). The shifts in the distribution of T_R/T_B cannot be clearly identified (Fig 9(g); Table 7).

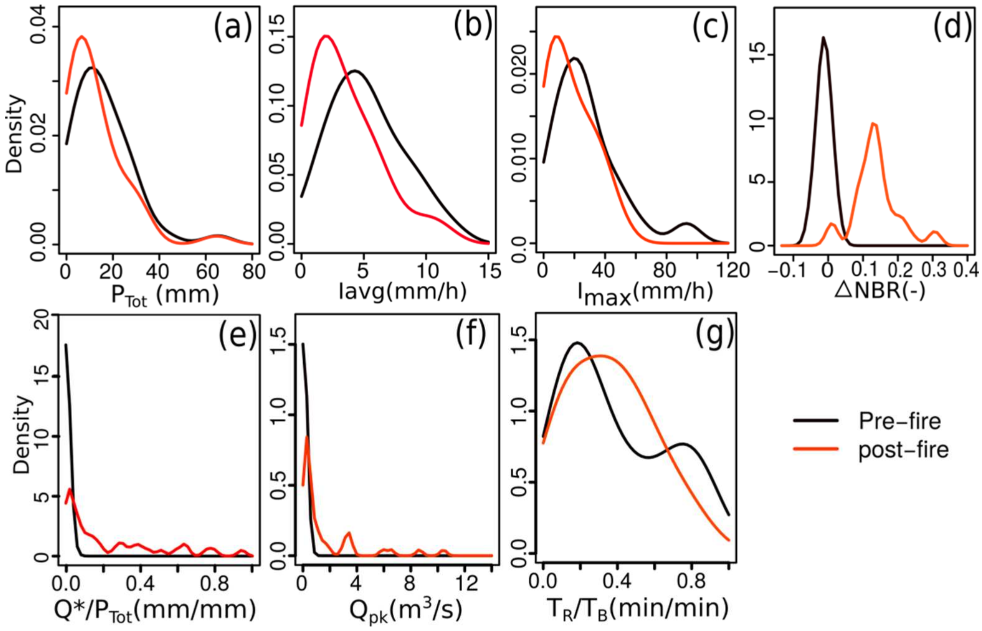

Figure 9: Density distributions comparison between pre (black) and post-fire (red) event-based precipitation (a) P_{Tot}, (b) I_{avg}, (c) I_{max}, (d) ΔNBR, and streamflow hydrograph (e) $Q*/P_{Tot}$, (f) Q_{pk} and (g) T_R/T_B, properties from samples of 38 events pre- and 38 post-fire. Please refer to Table 7 with Kolmogorov-Smirnov tests for pre- and post-fire distributions comparison.

Table 7: Kolmogorov-Smirnov test results for the distributions shown in Figure 9. The seven study variables (shown in Figure 9) are replicated in column 1 (i.e. Metric). The K-S maximum distance statistic (D) is presented in column 2. The null hypothesis H_0 is that the two series are drawn from the same distribution. The K-S theoretical threshold value for α=0.005 and n=38 is $D_{n,\alpha}$ = 0.276.

Metric	D	H_0
P_{Tot} (mm)	0.2368	Accept
I_{avg} (mm)	0.3421	Reject
I_{max} (mm)	0.2632	Accept
ΔNBR	0.9211	Reject
$Q*/P_{Tot}$ (mm/mm)	0.8947	Reject
Q_{pk} (m^3/s)	0.7632	Reject
T_R/T_B (min/min)	0.1579	Accept

Precipitation characteristics (i.e. P_{Tot}, I_{max}, I_{avg}) do not seem to be strongly correlated as shown by Figure C.1. The variance contribution results shown in Figure 10 and further detailed in Figure D.1 and Table D.1 help quantify the relationships between burn severity, precipitation properties and hydrologic response both pre- and post-fire. For the pre-fire events, precipitation-related predictors contribute in 98% (P_{Tot} and I_{avg}), 73% (P_{Tot} and I_{avg}) and 100% (P_{Tot} and I_{max}) to the total variability that is possible to explain of each predictand (Q^*/P_{Tot}, Q_{pk} and T_R/T_B; see Table D.1) when the four predictors are included within the best possible linear model combinations. Contrastingly, for the post-fire condition, and except for T_R/T_B, ΔNBR displaces all precipitation properties as the main driver of hydrologic response contributing 82% and 79% to the explained variability of Q^*/P_{Tot} and Q_{pk} respectively. Consistent to previous results, T_R/T_B remains mostly controlled by P_{Tot}.

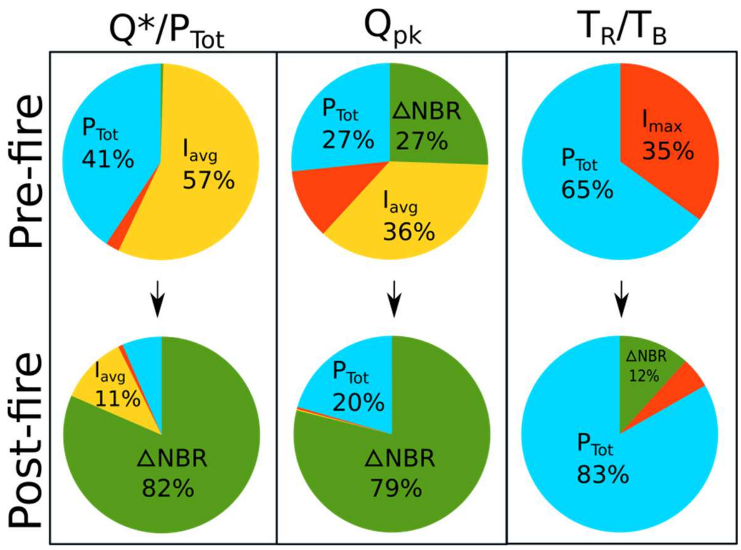

Figure 10: Results of the variance contribution analysis to identify the marginal contribution of each of the four predictors (i.e. I_{avg}, P_{Tot}, I_{max} and ΔNBR) to the explained variability of the three predictands (i.e. Q^*/P_{Tot}, Q_{pk} and T_R/T_B) pre- and post-fire. Please refer to Figure D.1 and Table D.1 to see the full results including all linear model combinations and the maximum percent of explained variance of each model.

At the inter-annual scale, burn scars undergo a recovery process with vegetation re-growth eventually leading to canopy densities similar to pre-fire conditions (in the absence of species replacement or succession), and as this process occurs a hysteresis effect on the values of Q/P_{Tot} is observed. Figure 11 illustrates this process through seasonal average Q/P_{Tot} plotted against the corresponding seasonal average ΔNBR throughout the inter-annual catchment's evaluation period.

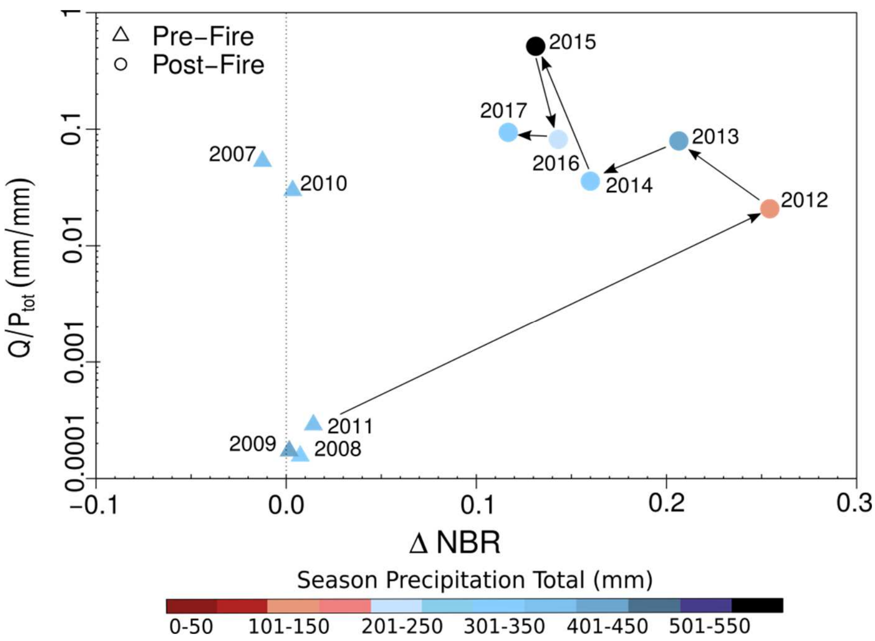

Figure 11: Seasonal Q/P_{Tot} vs. average ΔNBR for Camp Creek during six years before and six after the wildfire occurrence. Each season is classified by its total precipitation. Arrows connect the sequence of years post-fire to identify vegetation re-growth and runoff coefficient trends.

Figure 11 shows that the pre-fire years (2007 through 2011) present low values with ΔNBR ranging between -0.015 and 0.015 and relatively low Q/P_{Tot} values, except by 2007 and 2010. Between 2011 and the 2012 fire year, an increase in ΔNBR from 0.015 in 2011 to 0.26 in 2012 is associated with an increase in Q/P_{Tot} from 0.0003 to 0.02 in 2012 with this period being one of the driest in terms of low seasonal precipitation (i.e. 122 mm). The 2013 – 2017 seasonal sequence indicates a trend toward decreasing ΔNBR values, although runoff efficiencies remain higher than many of the pre-fire years shown.

5. Discussion

5.1 Evaluating post-fire hydrologic response shifts through NBR

Previous studies have described post-fire anomalies and their relation to remotely-sensed indices (Moody et al. 2008; Kinoshita and Hogue, 2011, Benyon et al. 2013, Moody et al. 2015). For example, Moody et al. (2008 and 2015) linked pre- and post-fire ΔNBR to short-term soil hydraulic alterations and anomalies in peak streamflows post-fire. Kinoshita and Hogue (2011) evaluated the annual evolution in runoff production of a burned watershed in California but using time series of the EVI. In an effort to quantify vegetation recovery, Jin et al. (2012) used multi-year times series of NBR to evaluate changes in forest albedo. The results presented in this manuscript represent the first effort to systematically evaluate the utility of NBR to reveal transient hydrologic catchment responses observed at multiple temporal scales (i.e. from event to inter-annual) for up to six years of vegetation regrowth.

In this study, catchment-scale hydrologic response to fire was evaluated for a large sample (i.e. 76) of precipitation events and seasonal totals that were similar to pre-fire values in an ephemeral, mountainous, forested catchment. A six-year, pre-fire time period provided a comparison timeframe to evaluate the shifts in hydrologic response at the watershed scale. Regarding the first research question, results showed that a drop in the catchment–average satellite-derived normalized burned ratio (NBR) is accompanied by an increase in the amount of effective runoff, contributing to larger magnitude streamflow responses in volume and peak flow rate suggesting a degree of coupling between burn severity and hydrologic response. Additionally, flow frequencies showed a consistent shift toward a larger range of exceedance probabilities post-fire, also indicating a slight decrease in the number of zero flow days with respect to the 20 years of record previous to the wildfire date in 2012. Previous studies had observed this effect from single events or a smaller sample of events (Stoof et al., 2012; Verdin et al., 2012; Young and Rust, 2012; Rosgen et al., 2013). The influence of burn severity on vegetation propagates from the minute to the inter-annual time scales indicating that the mechanisms of runoff generation endure for a significant period of time post-fire, regardless of the precipitation characteristics. The associated increases in volume and flow rates are suggestive of enhanced infiltration excess overland flow (Mayor et al., 2007). Three particular events in April and May of 2010 show large runoff efficiencies, similar to post-fire events. We hypothesize these could be due to a prolonged snow-melt period extending from late-April to early May. Out of the three evaluation metrics (i.e. Q^*/P_{Tot}, Q_{pk} and T_R/T_B), Q^*/P_{Tot} was the most significantly affected for all precipitation events post-fire. This means that the efficiency of runoff volume production is significantly enhanced regardless of the precipitation total from the storm to the seasonal scales. This result is similar to previous studies investigating fire impacts on stream hydrology. Kinoshita and Hogue (2015) also noted elevated streamflow during low flow seasons for up to 10 years post-fire, producing a newly perennial system. However, the increase in peak streamflow shown in Camp Creek's post-fire was not observed in Lane et al. (2006) or Kinoshita and Hogue (2015). The reasons both studies provide for this is the rapid breakdown or altogether absence of fire-induced soil hydrophobicity.

On the other hand, although Cydzic and Hogue (2009) found significant reductions in basin lag time for six large to moderate post-fire runoff events, attributing the change to reduced infiltration associated with loss of vegetation and increased imperviousness, the present study did not find significant changes in the time to peak flow relative to the total time base of the hydrographs. One reason for this could be the ephemeral condition of Camp Creek added to the relative small size of the catchment as compared to larger watersheds studied by Cydzic and Hogue.

In answering the second science question related to the utility of ΔNBR to quantify inter-annual runoff alterations and hydrologic recovery post-fire, the development of a variance contribution analysis provided further element tools to link satellite-derived burned severity to the observed shifts in hydrologic response. For the case of this single wildfire event, no direct mathematical relations were found to exactly predict the magnitude of expected change for particular combinations of ΔNBR, P_{Tot}, I_{max} or I_{avg}. Nonetheless, the cross-scale analyses conducted outlined that observed event-scale shifts in watershed stream response characteristics are found to shape longer-term runoff ratios post-wildfire. Further, post-fire vegetation recovery is a key determinant in the evolution of runoff as noted by Wittenberg et al. (2007), Casady et al. (2009) and Kinoshita and Hogue (2011) that conducted their analyses through time series of ΔEVI. We selected paired-basin ΔNBR as it removes the effects of phenology and enhances the distinction between burned and unburned surfaces with the addition of the mid-infrared spectral band. As ΔNBR decreased several months after the wildfire occurred, seasonal average runoff began recovering toward pre-fire values following a hysteresis pattern (see Figure 11) with the burn severity but also precipitation depth as exemplified by the exceptionally wet year of 2015. Very strong positive ENSO phases, like the one in 2015, enhance the effect of fire severity through significant increases in Q/P_{Tot} of up to, at least, one order of magnitude relative to runoff fractions during post-fire years. The Waldo Canyon fire was a rather severe wildfire judging by the long recovery time relative to normal-year hydrologic (e.g. non-ENSO; 2008, 2009, 2010) pre-fire conditions. We argue that this hysteresis effect rules post-fire hydrologic responses as measured by Q^*/P_{Tot} and possibly also Q_{pk}. The time and magnitude of such an effect depends on the severity of the burn and vegetation species pre- and post-fire. While a clear mathematical or statistical relationship between the ΔNBR, Q^*/P_{Tot} and Q_{pk} was not found, the balance of evidence shows correlation between hydrologic response properties and ΔNBR. The lack of identifying a clear relation can be attributed to the highly complex watershed response processes and their feedbacks that rule post-fire runoff responses. Additional factors include antecedent soil moisture conditions and snow processes, but also differences in soil hydraulic properties determined by the short-term presence of an ash layer (Woods and Balfour, 2010; Ebel et al., 2012). As noted by previous authors, post-fire event runoff generating processes and magnitudes are dynamic (Shakesby and Doerr, 2006; Larsen et al., 2009) and therefore cannot likely be captured by a single vegetation metric.

Although the results presented herein are based on a single basin's response, the study underlines the potential use of paired-basin ΔNBR for process understanding and predicting acute and chronic anomalies in vegetation and runoff and their linked recovery after a wildfire event. Along with precipitation characteristics and antecedent soil moisture conditions, NBR is useful in determining mean expected shifts in effective runoff and peak streamflow from the event to the inter-annual time scales. NBR can also be used to reveal the vegetation recovery pathway that restores hydrologic conditions (i.e. hysteresis curve), demonstrating its usability to track the evolution of the annual runoff anomalies relative to pre-fire conditions. Despite no straightforward relations being found between precipitation characteristics, antecedent soil moisture and burn severity, the findings of this study are of utility to hyper-resolution, process-based modelers (including the newly developed National Water Model (Gochis et al. 2018)) that account for time-evolving vegetation and land cover status. Linking satellite-derived indices to such hydrologic response metrics could also result in improvements of the rainfall-runoff hydrograph calculation methods (e.g. U.S. Natural Resources Conservation Service (SCS) method and/or unit and synthetic hydrographs) after a wildfire event. In an operational context, land managers and decision makers could rely on the usability of NBR and ΔNBR to better monitor, understand and estimate both event and long-term responses of burned watersheds, particularly those that are ungauged.

5.2 Study scope and limitations

Results provide consistent evidence of the exacerbated post-fire runoff responses and their occurrence from the hourly to the inter-annual time scales. However inherent uncertainties arise when taking a lumped approach to vegetation dynamics. For example, within-burn heterogeneity might play a role in enhancing or inhibiting water flow connectivity after fire. A distributed approach could help shed light on the post-fire vegetation dynamics of each sub-catchment, which might not be well captured by the catchment-average ΔNBR. Additionally, uncertainties are likely to influence results when three point-based rain gauges are applied to analyze catchment-scale streamflow dynamics. Spatially distributed, bias-corrected radar-based precipitation data is preferred when quantifying catchment scale streamflow dynamics because it provides an estimation of rainfall spatial variability with respect to the burned areas. Further, the present study did not explicitly consider the effects of the fire severity on the soil hydraulic properties as directly measured from the terrain. These results underscore the importance of in situ soil measurements and field validated data for storm-scale hydrologic projections.

6. Conclusions

Acute (short-term) and chronic (long-term, 6 years post-fire) transient streamflow shifts caused by wildfires are evaluated for a forested, mountain catchment under warm season precipitation. Along with the quantified shifts, the utility of the remotely sensed Normalized Burn Ratio (NBR) is explored and quantified from the event to inter-annual scales to study the transient post-fire changes in streamflow. Results can be summarized as:

1. Observed reductions in NBR due to wildfire are concurrent with increases in runoff production (i.e. Q^*/P_{Tot}) under similar event precipitation depths, intensities and antecedent soil moisture conditions.
2. Daily average flow duration curves show increases of an order of magnitude in the maximum streamflow values for the same exceedance probability events.
3. Increases in effective runoff (Q^*/P_{Tot}) and runoff fraction (Q/P_{Tot}) are observed at the event, daily, monthly, and seasonal scales for similar precipitation totals pre- and post-fire. The largest absolute increase in runoff production is observed at the event scale (Q^*/P_{Tot} increases in two orders of magnitude in average) indicating a significant shift in flash flood probability post-fire.

4. Of the three response hydrograph metrics, Q^*/P_{Tot} and Q_{pk} were the ones that illustrated the largest positive changes. This indicates that regardless of the precipitation type or intensity, enhanced runoff generation mechanisms were able to transform available precipitation into quick flow resulting in taller, wider response hydrographs. The response time was not necessarily identified as a critical shift variable in this catchment, meaning that travel and residence times may not necessarily be affected by wildfires on ephemeral catchments of this type.
5. Density distributions and K-S tests showed significant positive shifts for ΔNBR, Q^*/P_{Tot} and Q_{pk} post-fire, despite P_{Tot}, I_{avg}, I_{max} showed average decreases from a set of storm events analyzed post-fire.
6. A variance contribution analysis further supports the strong dependence of hydrologic responses on precipitation properties pre-fire, but ΔNBR was a primary contributor on post-fire hydrologic response.
7. A hysteresis effect was found at the inter-annual scale between the seasonal runoff fraction (i.e. Q/P_{Tot}), ΔNBR and P_{Tot} that illustrates the strong controls of soil and vegetation conditions on the corresponding runoff production at multiple temporal scales post-fire. For this particular case, 6 years of vegetation re-growth and soil hydraulic recovery post-fire are not enough time to return to pre-fire hydrologic conditions as the runoff mechanisms enhanced by the wildfire are still producing larger streamflow values comparable to pre-fire years with exceptional rainfall or snow seasons.

In summary, paired-basin ΔNBR was found to be of high utility for hydrologic analyses as it indicated vegetation status through its temporal correlation with the efficiency of runoff generation. This finding supports the hypothesis that the remotely-sensed ΔNBR could potentially be used to gain process understanding and improve predictions in burned basins as they are susceptible to yielding much greater runoff ratios than what is expected during pre-fire conditions. ΔNBR can also be used to monitor the basin's vegetation and hydrologic response recovery and improve transient modeling of the effects of vegetation status on hillslope and channel runoff. Future work could focus on conducting physically-based, distributed hydrologic observations and modeling to disaggregate the spatio-temporal variability of runoff-generating mechanisms that are responsible for the shifts observed across the temporal scales illustrated in this study.

Acknowledgements

This material is based upon work supported by the Army Research Laboratory and the Army Research Office under contract/grant number W911NF-18-1-0007 through the Young Investigator Program that funded Lead author Hernan Moreno and co-author Tri G. Pham. We also thank the editors Dr. Emmanouil Anagnostou and Dr. Tim McVicar, the associate editor Dr. Patrick N. Lane and the anonymous reviewers whose comments and suggestions significantly improved the quality of this manuscript.

Appendix A: Waldo Canyon Burn Scar

Areal extent of the Waldo Canyon wildfire obtained through the United States Forest Service (USFS) Remote Sensing Applications Center (Figure A.1). This classification indicates that Camp Creek watershed was primarily affected by moderate and high burn severities.

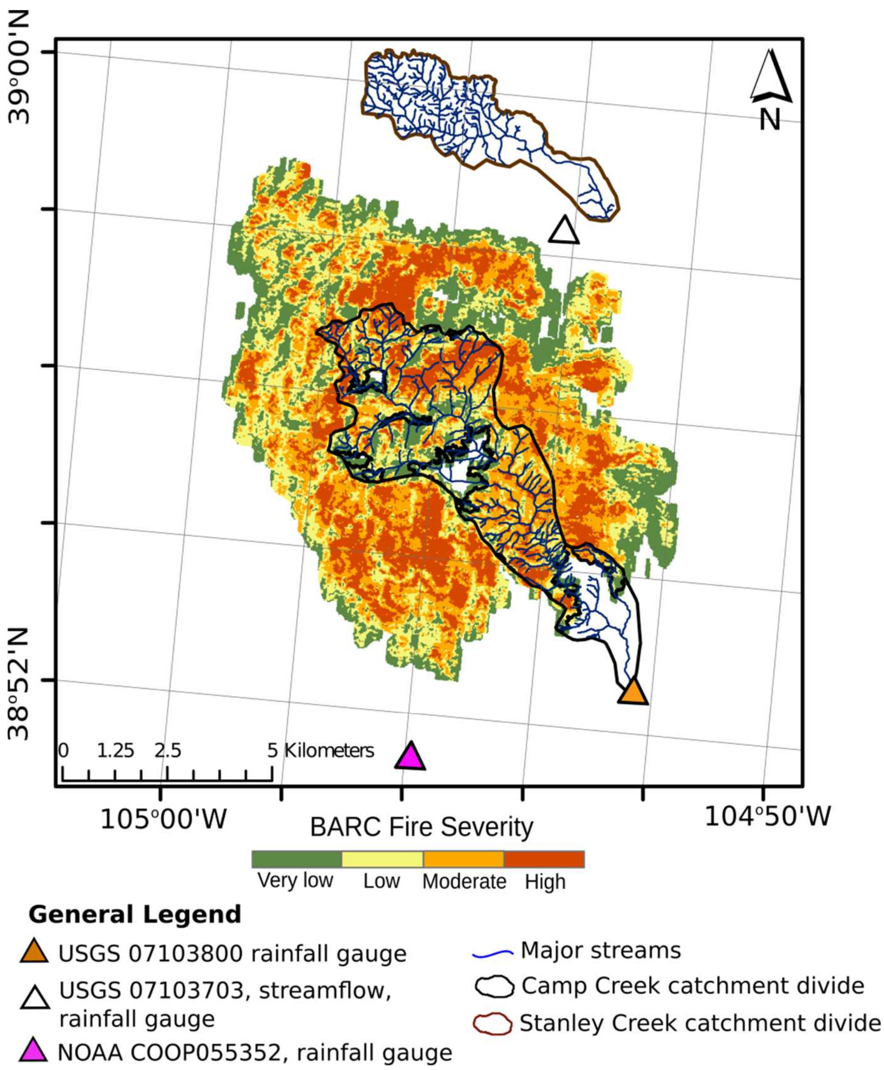

Figure A.1: Field validated burn severity according to the Burned Area Emergency Response (BAER) team for the Waldo Canyon Fire and accessed through the Remote Sensing Applications Center (RSAC) user interface.

Appendix B: Unburned, adjusted NBR values from control catchment

For the post-fire period, unburned values at Camp Creek are obtained from a linear regression with Stanley Creek, a neighboring, unburned catchment with similar vegetation cover and type and therefore spectral signature.

Table B.1: Regression models for simultaneous catchment average NBR values at Camp and Stanley Creek basins

Model	Expression	R^2
Linear	$NBR_{camp}=0.0228 + 0.7281NBR_{Stanley}$	0.80
Exponential	$NBR_{camp}=0.1 + e^{2.85941NBRStanley}$	0.76
Logarithmic	$NBR_{camp}=0.2408\ Ln(NBR_{Stanley})+0.5349$	0.80
Polynomial	$NBR_{camp}=-0.9476(NBR_{Stanley})^2+1.3786NBR_{Stanley}-0.0848$	0.80
Power	$NBR_{Camp}=0.7577(NBR_{Stanley})^{0.959}$	0.79

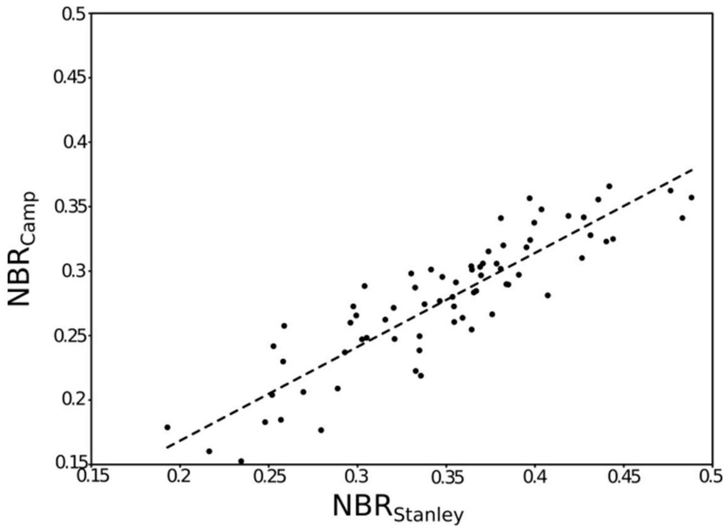

Figure B.1: Scatterplot of simultaneous catchment average NBR values at Camp (Y-axis) and Stanley (X-axis) Creek watersheds, and linear fit during pre-fire (2006-2012) conditions.

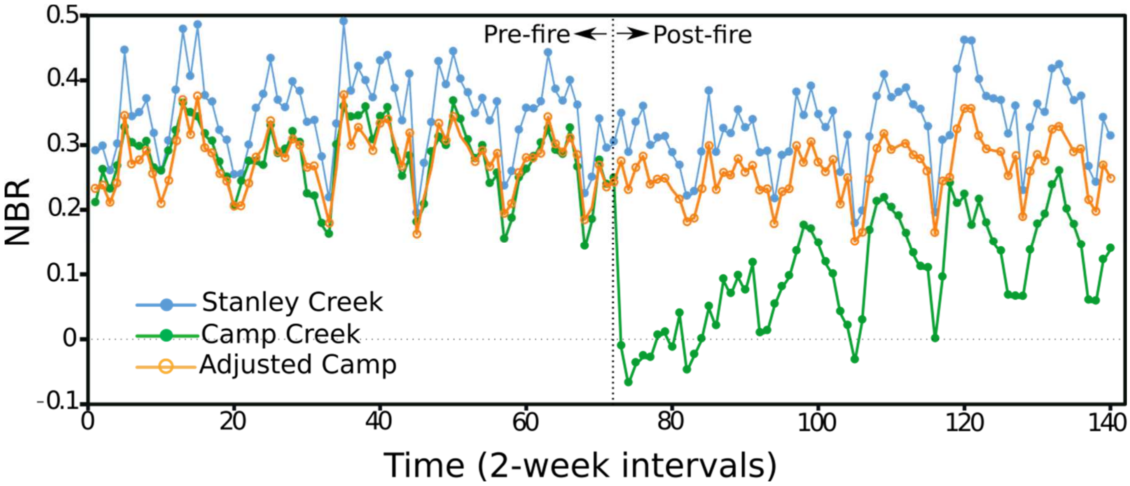

Figure B.2: Time series of biweekly, simultaneous catchment average NBR values at Stanley (unburned) and Camp (burned) creeks, along with the linearly adjusted time series at Camp Creek from the values at Stanley Creek. Values are only for the warm season of each year between 2006 and 2018.

Appendix C: Event precipitation characteristics pre- and post-fire in Camp Creek

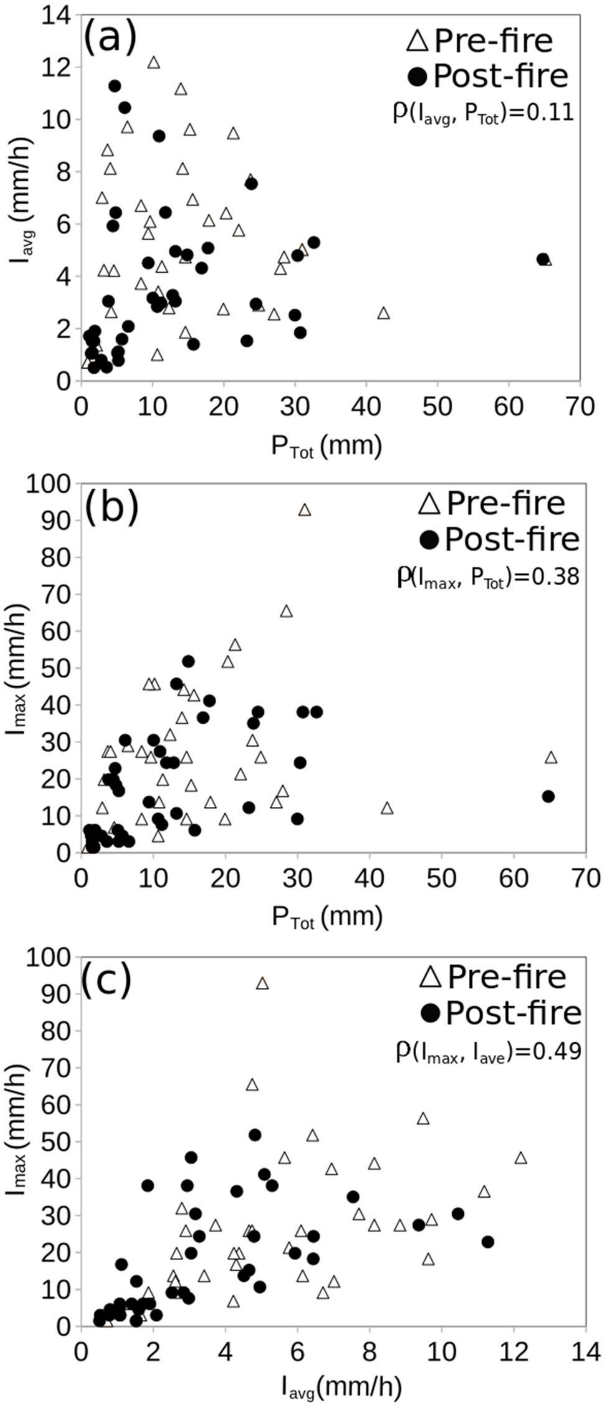

Figure C.1: Event-based scatterplots between (a) I_{avg} and P_{Tot}, (b) I_{max} and P_{Tot}, (c) I_{max} and I_{avg}, for 38 isolated precipitation events pre- (triangles) and 38 post- (circles) fire. Pearson correlation coefficients (ρ) are shown within each plot.

Appendix D: Variance contribution model results

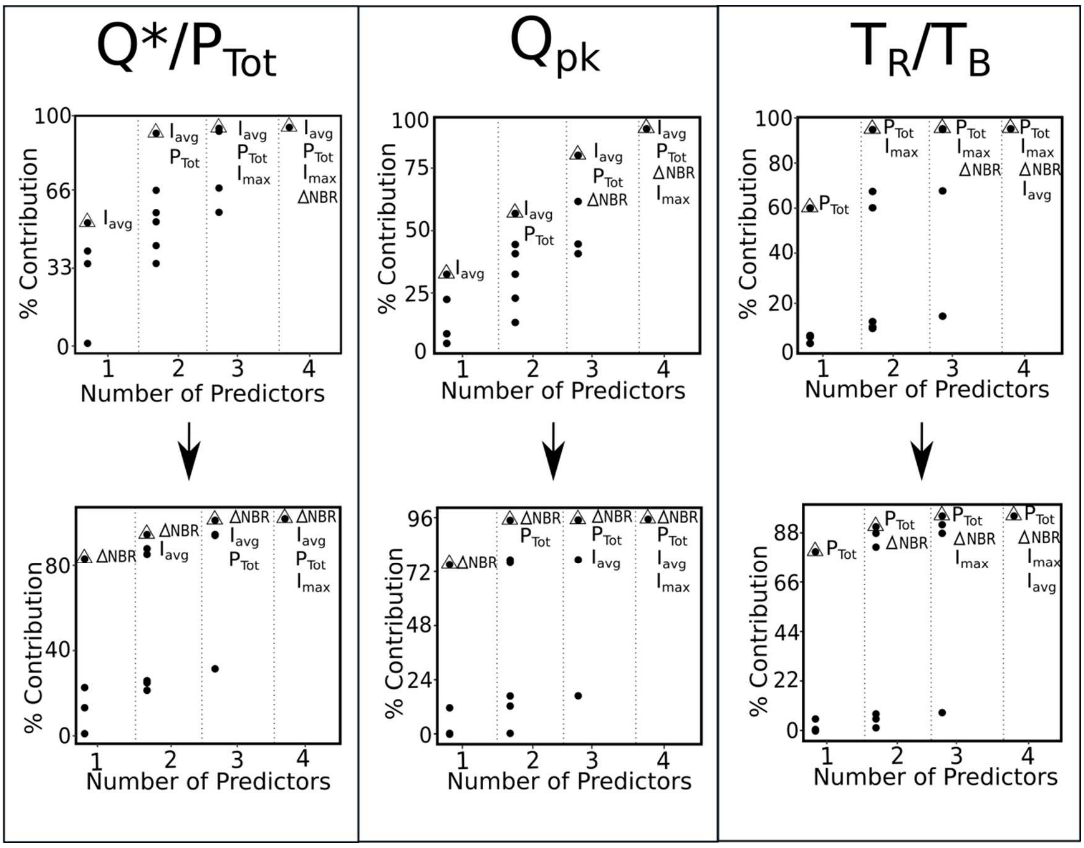

Figure D.1: Percent contribution of selected linear regression models to the variability of the predictands (i.e. Q^*/P_{Tot}, Qpk and T_R/T_B columns) when 1, 2, 3 and 4 predictors (i.e. I_{avg}, P_{Tot}, I_{max} and ΔNBR) are included in all possible linear combinations for pre- and post-fire (rows) events. Triangles indicate the best models for each number of predictors and their percent contribution to each of the predictands.

Table D.1: Coefficient of determination (R^2) as indicative of the fraction of explained variance between the best combination of the four predictors (see Figure D.1.) and each of the predictands for pre- and post-fire conditions.

	Q^*/P_{Tot}	Q_{pk}	T_R/T_B
Pre-fire	0.58	0.66	0.55
Post-fire	0.57	0.70	0.74

References

Akaike, H., 1973. Formation theory and an extension of the maximum likelihood principle. In B.N. Petrov & F. Csaki (Eds), *Second international symposium on information theory* (pp. 267-281). Budapest, HU: Akademiai Kiado.

Baker, D.B., Richards, R.P., Loftus, T.T., and Kramer, .J.W., 2004. A New Flashiness Index: Characteristics and Applications to Midwestern Rivers and Streams. *J. Am. Water Resour. Assoc.* 40 (2), 503-522.

Bart, R.R., 2016. A regional estimate of postfire streamflow change in California. *Water Resour. Res.* 52, 1465-1478. doi: 10.1002/2014WR016553.

Bart, R.R. and Hope, A., 2010. Streamflow response to fire in large catchments of a Mediterranean-climate region using paired-catchment experiments. *J. Hydrol.* 388, 370-378. doi:10.1016/j.jhydrol.2010.05.016

Benavides-Solorio, J., and MacDonald, L.H., 2001. Post–fire Runoff and Erosion from Simulated Rainfall on Small Plots, Colorado Front Range. *Hydrol. Process.* 15 (15), 2931-2952. doi: 10.1002/hyp.5017.

Benyon, R.G. and Lane, P.N.J., 2013. Ground and satellite-based assessments of wet eucalypt forest survival and regeneration for predicting long-term hydrological responses to a large wildfire. *For. Ecology Management* 294 197-207. doi: 10.1016/j.foreco.2012.04.003

Bosch, J.M. and Hewlett, J.D., 1982. A Review of Catchment Experiments to Determine the Effect of Vegetation Changes on Water Yield and Evapotranspiration. *J. Hydrol.* 55 3-23. doi: 10.1016/0022-1694(82)90117-2.

Brown, A.E., Zhang, L., McMahon, T.A., Western, A.W. and Vertessy, R.A., 2005. A review of paired catchment studies for determining changes in water yield resulting from alterations in vegetation. *J. Hydrol.* 310 28-61. doi: 10.1016/j.jhydrol.2004.12.010.

Burt, T.P. and Swank, W.T., 1992. Flow Frequency Response to Hardwood-to-Grass Conversion and Subsequent Succession. *Hydrol. Process.* 6 179-188. doi: 10.1002/hyp.3360060206.

Casady, G.M., Leeuwen, W.J.D., Marsh, S.E., 2010. Evaluating Post-Wildfire Vegetation Regeneration as a Response to Multiple Environmental Determinants. *Environ, Model. Assess.* 15 (5), 295-307. doi: 10.1007/s10666-009-9210-x.

Cerdà, A., 1998. Changes in Overland Flow and Infiltration after a Rangeland Fire in a Mediterranean Scrubland. *Hydrol. Process.* 12 (7), 1031-1042. doi: 10.1002/(SICI)1099-1085(19980615)12:7<1031::AID-HYP636>3.0.CO;2-V.

Cerdà, A. and Doerr, S.H., 2005. The Influence of Vegetation Recovery on Soil Hydrology and Erodibility Following Fire: An Eleven Year Investigation. *Int. J. Wildland Fire* 14 (4), 423-437. doi: 10.1071/WF05044.

Cerdà, A. and Lasanta, T., 2005. Long-Term Erosional Responses after Fire in the Central Spanish Pyrenees: 1. Water and Sediment Yield. *CATENA* 60 (1), 59-80. doi: 10.1016/j.catena.2004.09.006.

Chin, A., An, L., Florsheim, J.L., Laurencio, L.R., Marston, R.A., Solverson, A.P., Simon, G.L., Stinson, E., Wohl, E., 2016. Investigating feedbacks in human-landscape systems: Lessons following a wildfire in Colorado, USA. *Geomorphol.* 252 40-50. doi: 10.1016/j.geomorph.2015.07.030.

Cocke, A. E., Fulé, P. Z. and Crouse, J. E.. 2005. Comparison of burn severity assessments using Differenced Normalized Burn Ratio and ground data. *Int. J. of Wildland Fire*, 14, pp. 189-198.

Cydzik, K. and Hogue, T., 2009. Modeling Postfire Response and Recovery Using the Hydrologic Engineering Center Hydrologic Modeling System (HEC-HMS). *J. Am. Water Resour. Assoc*. 45 (3), 702-714.

DeBano, L.F., 2000. The Role of Fire and Soil Heating on Water Repellency in Wildland Environments: A Review. *J. Hydrol.* 231–232, 195–206. doi: 10.1016/S0022-1694(00)00194-3.

Diaz-Delgado, R. and Pons, X. 2001. Spatial patterns of forest fires in Catalonia (NE of Spain) along the period 1975-1995 Analysis of vegetation recovery after fire. *For. Ecol. Management.* 147 67-74. doi: 10.1016/S0378-1127(00)00434-5.

Ebel, B.A., Moody, J.A. and Martin, D.A., 2012. Hydrologic Conditions Controlling Runoff Generation Immediately after Wildfire. *Water Resour. Res.* 48 (3), W03529. doi: 10.1029/2011WR011470.

Epting, J., Verbyl, D. and Sorbel, B., 2005. Evaluation of remotely sensed indices for assessing burn severity in interior Alaska using Landsat TM and ETM+. *Rem. Sens. of Environment*, 96, pp. 228-239.

Escuin, S., R. Navarro, P. Fernandez, 2008. Fire severity assessment by using NBR (Normalized Burn Ratio) and NDVI (Normalized Difference Vegetation Index) derived from LANDSAT TM/ETM images. *Int. J. Remote Sens*. 29:1053-1073.

Fuka, D.R., Walter, M.T., Archibald, J.A., Steenhuis, T.S. and Easton, Z.M., 2014: EcoHydRology: A Community Modeling Foundation for Eco-Hydrology. R package version 0.4.12. https://CRAN.R-project.org/package=EcoHydRology

Gochis, D.J., Barlage, M., Dugger, A., FitzGerald, K., Karsten, L., McAllister, M., McCreight, J., Mills, J., RafieeiNasab, A., Read, L., Sampson, K., Yates, D., Yu, W. 2018. The WRF-Hydro modeling system technical description (V5.0). NCAR Technical Note. 107 Pages. Doi: 10.5065/D6J38RBJ.

Gottfried, G.J., Neary, D.G., Baker, M.B. Jr. and Ffolliott, P.F., 2003. Impacts of Wildfires on Hydrologic Processes in Forest ecosystems: Two Case Studies. In 'Proceedings, First Interagency Conference on Research in the Watersheds', 27-30 October 2003, Benson, AZ USDA Agricultural Research Service, 668-673.

Heath, J.T., Chafer, C.J., van Ogtrop, F.F. and Bishop, T.F.A., 2014. Post-wildfire recovery of water yield in the Sydney Basin water supply catchments: An assessment of the 2001/2002 wildfires. *J. Hydrol.* 519 1428-1440. doi: 10.1016/j.jhydrol.2014.09.033.

Heinze, G., Wallisch, C., Dunkler, D., 2018. Variable selection – A review and recommendations for the practicing statistitian. *Biom. J.* 60(3):431-449. Doi:10.1002/bimj.201700067.

Helvey, J.D., 1980. Effects of a North Central Washington Wildfire on Runoff and Sediment Production. *JAWRA.* 16 (4) 627-634. doi: 10.1111/j.1752-1688.1980.tb02441.x.

Huete, A., Didan, K., Miura, T., Rodriguez, E.P., Gao, X. and Ferreira, L.G. , 2002. Overview of the Radiometric and Biophysical Performance of the MODIS Vegetation Indices. *Remote Sens. of Environ.* 83 195-213.

Inbar, M., Tamir, M. and Wittenberg, L., 1998. Runoff and Erosion Processes after a Forest Fire in Mount Carmel, a Mediterranean Area. *Geomorphol.* 24 (1), 17-33. doi: 10.1016/S0169-555X(97)00098-6.

Jensen, J.R., 2004 *Introductory Digital Image Processing: A Remote Sensing Perspective*, third ed. Prentice Hall.

Jin, Y., Randerson, J.T., Goetz, S.J., Beck, P.S.A., Loranty, M.M. and Goulden, M.L., 2012. The influence of burn severity on postfire vegetation recovery and albedo change during early succession in North American boreal forests. *J. Geophys. Res.* 117, G01036 doi:10.1029/2011JG001886

Jonsson, P. and Eklundh, L., 2004. TIMESAT – a program for analyzing time-series of satellite sensor data. *Computers & Geosci.* 30, 833-845. doi: 10.1016/j.cageo.2004.05.006.

Jungerius, P.D. and ten Harkel, M.J., 1994. The effect of rainfall intensity on surface runoff and sediment yield in the grey dunes along the Dutch coast under conditions of limited rainfall acceptance. *CATENA* 23, 269-279.

Kean, J.W., Staley, D.M. and Cannon, S.H., 2011. In Situ Measurements of Post-Fire Debris Flows in Southern California: Comparisons of the Timing and Magnitude of 24 Debris-Flow Events with Rainfall and Soil Moisture Conditions. *J. Geophys. Res.* 116, F04019. doi:10.1029/2011JF002005.

Key, C.H. and Benson, C.N., 2006. Landscape Assessment (LA) Sampling and Analysis Methods. USDA Forest Service General Technical Report RMRS-GTR-164-CD.

Kinoshita, A.M. and Hogue, T.S., 2011. Spatial and Temporal Controls on Post-Fire Hydrologic Recovery in Southern California Watersheds. *CATENA* 87 (2) 240-252. doi: 10.1016/j.catena.2011.06.005.

Kinoshita, A.M. and Hogue, T.S., 2015. Increased dry season water yield in burned watersheds in Southern California. *Environ. Res. Lett.* 10 (1), 014003. doi: 10.1088/1748-9326/10/1/014003.

Kinoshita, A.M., Chin, A., Simon, G.L., Briles, C., Hogue, T.S., O'Dowd, A.P., Gerlak, A.K., Albornoz, A.U., 2016. Wildfire, water, and society: Toward integrative research in the "Anthropocene". *Anthr.* 16 16-27. doi: 10.1016/j.ancene.2016.09.001.

Kuczera, G., 1987. Prediction of water yield reductions following a bushfire in ash-mixed species eucalypt forest. *J. Hydrol.* 94 215-236. doi: 10.1016/0022-1694(87)90054-0.

Lane, P.N.J., Best, A.E., Hickel, K. and Zhang, L., 2005. The response of flow duration curves to afforestation. *J. Hydrol.* 310 253-265. doi: 10.1016/j.jhydrol.2005.01.006.

Lane, P.N.J., Sheridan, G.J. and Noske, P.J., 2006. Changes in Sediment Loads and Discharge from Small Mountain Catchments Following Wildfire in South Eastern Australia. *J. Hydrol.* 331 (3-4) 495-510. doi: 10.1016/j.jhydrol.2006.05.035.

Larson, I.J., MacDonald, L.H., Brown, E., Rough, D., Welsh, M.J., Pietraszek, J.H., Libohova, Z., Benavides-Solorio, J.D. and Schaffrath, K., 2009. Causes of Post-Fire Runoff and Erosion: Water Repellency, Cover, or Soil Sealing? *Soil Sci. Soc. Am. J.* 73 (4) 1393-1407. doi: 10.2136/sssaj2007.0432.

Lhermitte, S., Verbesselt, J., Verstraeten, W. W. and Coppin, P., 2010. A pixel based regeneration index using time series similarity and spatial context. *Photogrammetric Eng. Remote, Sens.* 76 (6) 673-682.

Loáiciga, H.A., Pedreros, D. and Roberts, D., 2001. Wildfire-Streamflow Interactions in a Chaparral Watershed. *Adv. Environ. Res.* 5 (3) 295-305. doi:10.1016/S1093-0191(00)00064-2.

Loboda, T. K.J. O'Neal, and I. Csiszar., 2007. Regionally adaptable dNBR-based algorithm for burned area mapping from MODIS data. Rem. Sens. of the Environment 109(4):429-442

MacDonald, L.H. and Huffman, E.L., 2004. Post-Fire Soil Water Repellency: Persistence and Soil Moisture Thresholds. *Soil Sci. Soc. Am. J.* 68 (5) 1729-1734.

Mahat, V., Silins, U. and Anderson, A., 2016. Effects of Wildfire on the Catchment Hydrology in Southwest Alberta. *CATENA* 147 51-60. doi: 10.1016/j.catena.2016.06.040.

Mahoney, K., Ralph, F.M., Wolter, K., Doesken, N., Dettinger, M., Gottas, D., Coleman, T. and White, A., 2015. Climatology of Extreme Daily Precipitation in Colorado and Its Diverse Spatial and Seasonal Variability. *J. Hydrometeorol.* 16 (2) 781-792. doi:10.1175/JHM-D-14-0112.1.

Matsushita, B., Yang, W., Chen, J., Onda, Y. and Qiu, G., 2007. Sensitivity of the Enhanced Vegetation Index (EVI) and Normalized Difference Vegetation Index (NDVI) to Topographic Effects: A Case Study in High-Density Cypress Forest. *Sens.* 7 2636-2651.

Mayor, A.G., Bautista, S., Llovet, J. and Bellot, J., 2007. Post-Fire Hydrological and Erosional Responses of a Mediterranean Landscape: Seven Years of Catchment-Scale Dynamics. *CATENA* 71 (1) 68-75. doi: 10.1016/j.catena.2006.10.006.

Miller, J.D. and A.E. Thode, 2007. Quantifying burn severity in a heterogeneous landscape with a relative version of the delta normalized burn ratio (dNBR). *Rem. Sens. of the Environment* 109(1):66-80.

Moench, R., 2002. Vegetative Recovery after Wildfire. Colorado State Forest Service. (Available: http://static.colostate.edu/client-files/csfs/pdfs/06307.pdf (Accessed September 2017).

Moody, J.A. and Martin, D.A., 2001a. Post-Fire, Rainfall Intensity–peak Discharge Relations for Three Mountainous Watersheds in the Western USA. *Hydrol. Process.* 15 (15) 2981-2993. doi: 10.1002/hyp.386.

Moody, J.A. and Martin, D.A., 2001b. Initial Hydrologic and Geomorphic Response Following a Wildfire in the Colorado Front Range. *Earth Surf. Process. Landf.* 26 (10) 1049-1070. doi:10.1002/esp.253.

Moody, J.A., Martin, D.A., Haire, S.L. and Kinner, D.A., 2008. Linking Runoff Response to Burn Severity after a Wildfire. *Hydrol. Process.* 22 (13) 2063-2074. doi: 10.1002/hyp.6806.

Moody, J.A., Ebel, B., Nyman, P., Martin, D., Stoof, C., and R. McKinley, 2015. Relations between soil hydraulic properties and burn severity. *Int. J. Wildland Fire.* 25 279-293.

Moody, J.A., and Ebel, B.A., 2014. Infiltration and Runoff Generation Processes in Fire-Affected Soils. *Hydrol. Process.* 28 (9) 3432-3453. doi:10.1002/hyp.9857.

Moreno, H.A.**,** Vivoni, E.R., and Gochis, D.J., 2012. Utility of quantitative precipitation estimates for high resolution hydrologic forecasts in mountain watersheds of the Colorado Front Range. *J. Hydrol.* 438-439, 66-83. doi:10.1016/j.jhydrol.2012.03.019.

Moreno, H.A., Vivoni, E.R., and Gochis, D.J., 2013. Limits to flood forecasting in the Colorado Front Range for two summer convection periods using radar nowcasting and a distributed hydrologic model. *J. Hydrometeorol.* 14, 1075-1097. doi:10.1175/JHM-D-12-0129.1.

Moreno, H.A., Gupta, H.V., White, D.D. and Sampson, D.A., 2016. Modeling the distributed effects of forest thinning on the long-term water balance and streamflow extremes for a semi-arid basin in the southwestern US. *Hydrol. Earth Syst. Sci.* 20 1241-1267. doi: 10.5194/hess-20-1241-2016.

NASA LP DAAC, 2000, MOD13Q1. Version 6. NASA EOSDIS Land Processes DAAC, USGS Earth Resources Observation and Science (EROS) Center, Sioux Falls, South Dakota (https://lpdaac.usgs.gov), accessed April 01, 2016, at https://earthexplorer.usgs.gov/

Nathan, R.J. and McMahon, T.A., 1990. Evaluation of Automated Techniques for Base Flow and Recession Analysis. *Water Resour. Res.* 26 (7) 1465-1473.

Neary, D.G., Ffolliott, P.F. and Landsberg, J.D., 2005. Wildland Fire in Ecosystems: Effects of Fire on Soil and Water. General Technical Report RMRS-GTR-42, vol. 4. United States Department of Agriculture, Forest Service, Rocky Mountain Research Station. Ogden, Utah 250 pp.

Olejnik, S., Mills, J. Keselman, H., 2000. Using Wherry's adjusted R^2 and Mallow's C_p for model selection from all possible regressions. The Journal of Experimental Education, 68:4, 365-380, doi: 10.1080/00220970009600643

Onda, Y., Dietrich, W.E. and Booker, F., 2008. Evolution of overland flow after a severe forest fire, Point Reyes, California. *CATENA* 72 (1) 13-20. doi: 10.1016/j.catena.2007.02.003.

Pierson, F.B., Robichaud, P.R. and Spaeth, K., 2001. Spatial and temporal effects of wildfire on the hydrology of a steep rangeland watershed. *Hydrol. Process.* 15 2905-2916. doi:10.1002./hyp.381.

Roy, D.P., Boschetti, L., Trigg, S.N., 2006. Remote Sensing of Fire Severity: Assessing the Performance of the Normalized Burn Ratio. *IEEE Geosci. Remote Sens. Lett.* **3** (1) 112-116.

Rosgen, D., Rosgen, B., Collins, S., Nankervis, J. and Wright, K., 2013. Waldo Canyon Fire Watershed Assessment: The WARSS Results. Coalition for the Upper South Platte, Lake George, CO, USA (Available: http://www.cusp.ws/wp-content/uploads/2014/10/1.WaldoCanyonFireAssessmentReport.pdf (accessed September 2017)).

Shakesby, R.A. and Doerr, S.H., 2006. Wildfire as a Hydrological and Geomorphological Agent. *Earth-Sci. Rev.* 74 (3-4) 269-307. doi: 10.1016/j.earscirev.2005.10.006.

Shin, S.S., Park, S.D. and Lee, K.S., 2013. Sediment and Hydrological Response to Vegetation Recovery Following Wildfire on Hillslopes and the Hollow of a Small Watershed. *J. Hydrol.* 499 154-166. doi: 10.1016/j.jhydrol.2013.06.048.

Smakhtin, V.U., 2001. Low flow hydrology: a review. *J. Hydrol.* 240 147-186. doi: 10.1016/S0022-1694(00)00340-1.

Staley, D.M., Gartner, J.E. and Kean, J.W. Objective Definition of Rainfall Intensity-Duration Thresholds for Post-fire Flash Flood and Debris Flows in the Area Burned by the Waldo Canyon Fire, Colorado, USA. Lollino, G., Giordan, D., Crosta, G.B., Corominas, J., Azzam, R., Wasowski, J., Sciarra, N. (Eds.), Engineering Geology for Society and Territory, Volume 2, Springer International Publishing (2015) 621-624 pp.

Stoof, C.R., Vervoort, R.W., Iwema, J., Elsen, E., Ferreira, A.J.D. and Ritsema, C.J., 2012. Hydrological Response of a Small Catchment Burned by Experimental Fire. *Hydrol. Earth. Syst. Sci.* 16 267-285. doi: 10.5194/hess-16-267-2012.

Uyeda, K.A., Stow, D.A., Roberts, D.A. and Riggan, P.J., 2017. Combining ground-based measurements of MODIS-based spectral vegetation indices to track biomass accumulation in post-fire chaparral. *Int. J. Remote Sens.* 38 (3) 728-741. doi: 10.1080/01431161.2016.1271477.

Veraverbeke, S., Lhermitte, S., Verstraeten, W.V. and Goossens, R., 2010. The temporal dimension of differenced Normalized Burn Ratio (dNBR) fire/burn severity studies: The case of the large 2007 Peloponnese wildfires in Greece. *Remote Sens. Environ.* 114 (11) 2548-2563.

Verdin, K.L., Dupree, J.A. and Elliott, J.G. Probability and volume of potential postwildfire debris flows in the 2012 Waldo Canyon Burn Area near Colorado Springs, Colorado: U.S. Geological Survey Open-File Report 2012-1158, 8p.

Walsh, R.P.D., Boakes, D.J., Coelho, C.O.A., Gonçalves, A.J.B., Shakesby, R.A. and Thomas, A.D., 1994. Impact of Fire-Induced Water Repellency and Post-Fire Forest Litter on Overland Flow in Northern and Central Portugal. In *Proceedings of the Second International Conference on Forest Fire Research*, II:1149-1159. Coimbra, Portugal.

Walz, Y., Maier, S.W., Dech, S.W., Conrad, C., and Colditz, R.R. 2007. Classification of burn severity using Moderate Resolution Imaging Spectroradiometer (MODIS): A case study in the jarrah-marri forest of southwest Western Australia, *J. of Geophys. Res*. 112, G02002.

Watt, W.E. and Chow, K.C.A., 1985. A general expression for basin lag time. *Can, J, Civ. Eng.* 12 294-300. doi: 10.1139/l85-031.

Weier, J. and Herring, D. "Measuring Vegetation (NDVI & EVI)." *Earth Observatory*. 30 Aug. 2000, accessed September 4, 2017 at https://earthobservatory.nasa.gov.

Weber, K.T., Seefeldt, S., Moffet, C. and Norton, J., 2008. Comparing fire severity models from post-fire and pre/post-fire differenced imagery. *GIScience and Remote Sensing* 45(4):392-405.

Wine, M.L. and Cadol, D., 2016. Hydrologic effects of large southwestern USA wildfires significantly increase regional water supply: fact or fiction? *Environ. Res. Lett.* 11 085006. doi: 10.1088/1748-9326/11/8/085006.

Wittenberg, L., Malkinson, D., Beeri, O., Halutzy, A. and Tesler, N., 2007. Spatial and Temporal Patterns of Vegetation Recovery Following Sequences of Forest Fires in a Mediterranean Landscape, Mt. Carmel Israel. *CATENA* 71 (1) 76-83. 10.1016/j.catena.2006.10.007.

Woods, S.W. and Balfour, V.N., 2010. The effects of soil texture and ash thickness on the post-fire hydrological response from ash covered soils. *J. Hydrol.* 393 (3-4) 274-286. doi: 10.1016/j.jhydrol.2010.08.025

Woodsmith, R.D., Vache, K.B., McDonnell, J.J. and Helvey, J.D., 2004. Entiat experimental forest: catchment-scale runoff data before and after a 1970 wildfire. *Water Resour. Res.* 40 W11701. doi:10.1029/2004WR003296

Young, D. and Rust, B., 2012. Waldo Canyon Fire – burned area emergency response soil resource assessment. USDA Forest Service, Region 5, Redding, CA, USA

Zhou, Y., Zhang, Y., Vaze, J., Lane, P. and Xu, S., 2015. Impact of bushfire and climate variability on streamflow from forested catchments in southeast Australia. *Hydrol. Earth Syst. Sci. Discuss.* 10 4397-4437. doi: 10.5194/hessd-10-4397-2013.